Development/Plasticity/Repair

The CB_1 Cannabinoid Receptor Drives Corticospinal Motor Neuron Differentiation through the Ctip2/Satb2 Transcriptional Regulation Axis

Javier Díaz-Alonso,[1,2] Tania Aguado,[1,2] Chia-Shan Wu,[3] Javier Palazuelos,[1,2] Clementine Hofmann,[4,5] Patricia Garcez,[6] François Guillemot,[6] Hui-Chen Lu,[3] Beat Lutz,[4] Manuel Guzmán,[1,2] and Ismael Galve-Roperh[1,2]

[1]Research Network Center for Biomedical Research in Neurodegenerative Diseases (CIBERNED), 28049 Madrid, Spain, [2]Department of Biochemistry and Molecular Biology I, Ramón y Cajal Institute of Health Research and Neurochemistry Research Institute, Complutense University, 28040 Madrid, Spain, [3]The Cain Foundation Laboratories, Jan and Dan Duncan Neurological Research Institute, Department of Pediatrics, Baylor College of Medicine, Houston, Texas 77030, [4]Institute of Physiological Chemistry, Medical Center of the Johannes Gutenberg University Mainz, 55128 Mainz, Germany, [5]Focus Program Translational Neuroscience, Johannes Gutenberg University, 55131 Mainz, Germany, and [6]Division of Molecular Neurobiology, National Institute of Medical Research, London, NW7 1AA, United Kingdom

The generation and specification of pyramidal neuron subpopulations during development relies on a complex network of transcription factors. The CB_1 cannabinoid receptor is the major molecular target of endocannabinoids and marijuana active compounds. This receptor has been shown to influence neural progenitor proliferation and axonal growth, but its involvement in neuronal differentiation and the functional impact in the adulthood caused by altering its signaling during brain development are not known. Here we show that the CB_1 receptor, by preventing Satb2 (special AT-rich binding protein 2)-mediated repression, increased Ctip2 (COUP-TF interacting protein 2) promoter activity, and Ctip2-positive neuron generation. Unbalanced neurogenic fate determination found in complete $CB_1^{-/-}$ mice and in glutamatergic neuron-specific *Nex*–$CB_1^{-/-}$ mice induced overt alterations in corticospinal motor neuron generation and subcerebral connectivity, thereby resulting in an impairment of skilled motor function in adult mice. Likewise, genetic deletion of CB_1 receptors in *Thy1–YFP–H* mice elicited alterations in corticospinal tract development. Altogether, these data demonstrate that the CB_1 receptor contributes to the generation of deep-layer cortical neurons by coupling endocannabinoid signals from the neurogenic niche to the intrinsic proneurogenic Ctip2/Satb2 axis, thus influencing appropriate subcerebral projection neuron specification and corticospinal motor function in the adulthood.

Introduction

The development of the cerebral cortex involves the sequential formation and specification of the excitatory neuron populations that constitute the definitive six-layered cortical structure (Molyneaux et al., 2007; Fishell and Hanashima, 2008). Among the cell intrinsic mechanisms involved in corticogenesis, a complex proneurogenic transcription factor program is responsible for the correct establishment of neuronal identity within an area or layer (Guillemot et al., 2006; Molyneaux et al., 2007). These factors coordinate cell-cycle exit, neuronal migration, and the specific gene expression program that dictates neuronal identity of upper and deep cortical neurons and axonal connectivity. Neurons projecting to subcortical areas are primarily located in early-generated deep layers 5 and 6, whereas callosal projecting neurons are abundant in upper layers 2 through 4 (Sur and Rubenstein, 2005; Molyneaux et al., 2007). Specification of subcortical (i.e., corticothalamic and subcerebral) projection neurons relies on the combinatorial action of a transcriptional regulation network composed of different factors, such as special AT-rich sequence-binding protein 2 (Satb2), chicken ovoalbumin upstream promoter transcription factor I (COUP-TFI), and its interacting protein 2 (Ctip2/Bcl11b), a zinc finger transcriptional repressor (Arlotta et al., 2005; Alcamo et al., 2008; Tomassy et al., 2010). Forebrain embryonic zinc finger-like protein 2 (Fezf2) and its downstream regulator COUP-TF interacting protein 2 (Ctip2) are sufficient to induce ectopic specification of subcerebral projection neurons, and, in particular, of corticospinal motor neurons (CSMNs), which reside in layer 5b and extend their axons to the spinal cord (Molyneaux et al., 2005; Chen et al., 2008). In contrast, upper-layer specification factor Satb2 directly

Received Feb. 11, 2012; revised Sept. 7, 2012; accepted Sept. 16, 2012.

Author contributions: J.D.-A., T.A., F.G., M.G., and I.G.-R. designed research; J.D.-A., T.A., C.-S.W., J.P., C.H., and P.G. performed research; J.D.-A., T.A., F.G., H.-C.L., B.L., M.G., and I.G.-R. analyzed data; J.D.-A., H.-C.L., B.L., M.G., and I.G.-R. wrote the paper.

This work was supported by Ministry of Science and Innovation Grants PLE2009-0117 (I.G-R.) Fundación Alicia Koplowitz (I.G.-R.), and SAF2009-08403 (M.G.), Community of Madrid–Complutense University of Madrid Grants S2011/BMD-2308, S2011/BMD-2336, and 950344 (M.G., I.G.-R.), National Institutes of Health Grants DA029381, HD065561, and NS048884 (H.-C.L.), and German Research Foundation Grant FOR926 (B.L.). J.D.-A. is supported by the Health Research Fund (PFIS), and T.A. and J.P. are supported by the Ministry of Science and Innovation. We are grateful to our collaborators that kindly contributed to this work by sharing reagents and molecular probes. We are also indebted to E. García-Taboada, E. Resel, M. Purrio, and A. Conrad for excellent experimental assistance and to A. González, A. García-Rodríguez, K. Mackie, O. Marín, and J. Ramírez-Franco for valuable comments.

Correspondence should be addressed to Ismael Galve-Roperh, Department of Biochemistry and Molecular Biology I, School of Biology, Complutense University, 28040 Madrid, Spain. E-mail: igr@quim.ucm.es.

DOI:10.1523/JNEUROSCI.0681-12.2012

 0270-6474/12/3216651-15$15.00/0

binds to matrix attachment regions (MARs) of the Ctip2 promoter and prevents Ctip2 expression, thus favoring the neuronal fate of callosal projection (Alcamo et al., 2008).

In addition to these endogenous determinants, an array of extracellular cues from the neurogenic niche is necessary for the precise coordination of cortical development. The endocannabinoid (eCB) system, via the cannabinoid CB_1 receptor, has been shown to exert a regulatory role in corticogenesis (Aguado et al., 2005; Berghuis et al., 2007; Morozov et al., 2009). Specifically, CB_1 receptor inactivation leads to defective ventricular/subventricular zone (VZ/SVZ) progenitor cell proliferation and axonal guidance alterations (Aguado et al., 2005; Mulder et al., 2008), thus impairing long-range corticothalamic connectivity (Mulder et al., 2008; Wu et al., 2010). However, the molecular mechanism of CB_1 receptor action in neuronal specification has not yet been investigated. Likewise, the impact on cortical development and the subsequent alterations in adult brain function as a consequence of altered prenatal CB_1 receptor function on intake of cannabinoid receptor agonists or antagonists by pregnant women remains primarily elusive (Galve-Roperh et al., 2009; Jutras-Aswad et al., 2009; Schneider, 2009). Hence, in the present study, we investigated the regulatory role of the CB_1 receptor in the transcription factor program that controls pyramidal neurogenesis and laminar differentiation, as well as its potential additional impact for adulthood neural functions. Our findings reveal that CB_1 receptor signaling, by modulating the Ctip2/Satb2 transcriptional regulatory code in differentiating neurons, controls neuronal projection fate differentiation, thereby tuning subsequent CSMN development and function.

Materials and Methods

Materials. The following materials were kindly donated: anti-CB_1 receptor antibody (K. Mackie, Indiana University, Bloomington, IN), $FAAH^{-/-}$ mice (B. Cravatt, Scripps Institute, San Diego, CA), pCAG–DsRed (M. Nieto, National Center of Biotechnology, Madrid, Spain), pfosluc constructs with the MAR sequences A2–A5 of the Ctip2 promoter and pMSCV–Satb2 expression vector (R. Grosschedl, Max Planck Institute of Immunobiology and Epigenetics, Freiburg, Germany), and HU-210 [(6a*R*,10a*R*)-3-(1,1′-dimethylheptyl)-6a,7,10,10a-tetrahydro-1-hydroxy-6,6-dimethyl-6*H*-dibenzo[b,d]pyran-9-methanol] (R. Mechoulam, Hebrew University, Jerusalem, Israel). Rat monoclonal anti-5-bromo-2′-deoxyuridine (BrdU), rabbit polyclonal anti-Ctip2, anti-T-box brain 1 (Tbr1), anti-Tbr2, and mouse monoclonal anti-Satb2 antibodies were from Abcam. Rabbit polyclonal anti-CB_1 antibody (Frontier Institute, Hokkaido, Japan), mouse monoclonal anti-CRE (Covance), mouse monoclonal anti-GFP (Invitrogen), and chicken polyclonal anti-GFP (Millipore) antibodies were also used.

Animals. Experimental designs and procedures were approved by the Complutense University Animal Research Committee in accordance with Directive 86/609/EU of the European Commission. All efforts were made to minimize the number of animals and their suffering throughout the experiments. Mice were maintained in standard conditions, keeping littermates grouped in breeding cages, at a constant temperature (20 ± 2°C) on a 12 h light/dark cycle with food and water *ad libitum*. The generation and genotyping of $CB_1^{-/-}$, $CB_1^{f/f,Nex\text{–}Cre}$, $CB_1^{f/f,Dlx5/6\text{-}Cre}$, and $FAAH^{-/-}$ mice and their respective littermate controls have been reported previously and was performed accordingly (Cravatt et al., 2001; Marsicano et al., 2003; Monory et al., 2007; Massa et al., 2010). Thy1–eYFP (line H) mice were obtained from The Jackson Laboratory [B6.Cg–Tg(Thy1–YFP–H)2Jrs/J] and crossed with $CB_1^{-/-}$ mice. The heterozygous F1 generation was crossed again with $CB_1^{-/-}$ mice. Mouse tissues of either sex were obtained during timed mating as assessed by vaginal plug.

Immunofluorescence and confocal microscopy. Coronal brain slices (10 μm) were processed as described previously (Mulder et al., 2008), and layers were identified by their discrete cell densities as visualized by Hoechst 33528 (Sigma) and β-III-tubulin counterstaining. After blockade with 5% goat serum, brain sections were incubated overnight at 4°C with the indicated primary antibodies. Confocal fluorescence images were obtained in a blinded manner by an independent observer, and all quantifications were obtained from a minimum of six sections from 1-in-10 series per mice. Immunofluorescence of cortical sections was performed along the rostral-to-caudal axis, and the quantifications were performed in the mediolateral area of rostromedial sections that correspond to the motor/somatosensory cortex. Pyramidal layer specification was determined at embryonic day 16.5 (E16.5), postnatal day 2 (P2), and P8 in a 50-μm-wide cortical column divided into 10 equally sized bins, from the ventricular surface to the marginal zone. At least two independent cortical columns were analyzed per section, and results were averaged (see Figs. 1, 2, 6, 8). Positive cells for the corresponding markers were quantified and referred to the total cell number in the bin identified by Hoechst 33528.

Protein kinase Cγ immunohistochemistry. Protein kinase Cγ (PKCγ) immunohistochemistry was performed in 100-μm-thick sagittal sections. After permeabilization, quenching of endogenous peroxidase activities and blockade with goat serum free-floating sections were incubated with rabbit anti-PKCγ antibody (Santa Cruz Biotechnology) and processed according to the instructions of the manufacturer with 1:500 goat biotinylated anti-rabbit IgG and with avidin-biotinylated peroxidase complex (ABC Standard Vectastain ABC kit; Vector Laboratories). Stained sections were mounted, and bright-field images were captured from an Olympus BX51 upright microscope using an Olympus DP70 CCD camera.

In situ *hybridization.* Coronal paraffin sections (10 μm) of E12.5, E13.5, E14.5, and E16.5 heads were obtained, deparaffinized, and processed for *in situ* hybridization as described previously (Monory et al., 2007). Clim1 (National Center for Biotechnology Information reference sequence NM_ 010698.3) riboprobe for *in situ* hybridization was amplified with the following primers: forward, ACCCTCATTCCCCGTTATT; and reverse, TGGCTCTCCTACCACCATC.

Real-time quantitative PCR. RNA was isolated using RNeasy Plus kit (Qiagen). cDNA was obtained with Transcriptor (Roche). Real-time quantitative PCR assays were performed using the FastStart master mix with Rox (Roche), and probes were obtained from the Universal Probe Library Set (Roche). Amplifications were run in a 7900 HT-Fast Real-Time PCR System (Applied Biosystems). Each value was adjusted by using 18S RNA and β-actin levels as reference.

Ex vivo *and* in utero *electroporation. Ex vivo* electroporation experiments were performed at E13.5 as described previously (Mulder et al., 2008) with pCAG–GFP and pCAG–CB_1–GFP expression vectors, or pGFP-V-RS (Origene) shControl and shCB_1 and dissociated cells were cultured as described below. In addition, $CB_1^{f/f}$ cortices were electroporated with pCAG–GFP or pCAG–Cre–GFP (Addgene). In addition, *in utero* electroporations were performed at E14.5 or E13.5 with pCAG–CB_1–GFP or DsRed (respectively) and analyzed at E16.5 (see Figs. 1*I*,*J*, 7*A*–*D*). *In utero* electroporation experiments with pCAG–CRE–GFP and pCAG-GFP control plasmids were also performed from E12.5 to P0 in $CB_1^{f/f}$ mice (see Fig. 4*D*,*E*).

Pyramidal and organotypical cortical cell cultures. Cortical neural progenitors were cultured from dissected cortices isolated at E13.5. Cells were mechanically dissociated and plated in polylysine- and laminin-coated dishes after *ex utero* electroporation and dissection of the cortical electroporated area (fast green positive). The neuronal phenotype was assessed after 7 d *in vitro* by quantification of Ctip2 and Satb2 expression in GFP-positive (GFP^+) cells from ≥10 randomly selected view fields/coverslip after Hoechst 33528 cell counterstaining in genetically manipulated cells. In addition, pharmacological regulation experiments were performed in wild-type (WT) brain slices.

Gene promoter activity assays. The neural stem cell line HiB5 was used after transient transfection with 0.75 μg of the A4- or A3–MAR–pfosluc reporter of the Ctip2 promoter, 0.5 μg of pCAG–CB_1–GFP, 0.25 μg of pMSCV–Satb2, and 0.02 μg of renilla-derived luciferase as internal transfection control with Lipofectamine 2000. Transcriptional promoter-driven luciferase activity was performed using the Dual-Luciferase Reporter Promega assay system and renilla-derived luciferase activity as internal transfection control in a Lumat LB9507 luminometer (Berthold Technologies). Control experi-

ments were performed with an excess of Satb2 expression that was able to efficiently block the Ctip2-reporter activity (data not shown).

Behavioral analyses. $CB_1^{-/-}$ and *Nex–*$CB_1^{-/-}$ mice and their respective wild-type littermates (WT and $CB_1^{f/f}$) were analyzed at 8 weeks of age with paired mean age among groups. Animals were always tested during the same light phase and acclimatized to the testing room for at least 30 min. All tests were video recorded for subsequent analysis and double-blind quantification. Mice were food deprived the night before the testing day (mean body weight at the end of the test becoming 92.6 ± 2.2% of the initial body weight). Skilled motor test and patch removal tasks were performed according to established protocols (Tomassy et al., 2010). Briefly, a Plexiglas reaching box (20 cm long × 8 cm wide × 20 cm high), with a 1-cm-wide vertical slit in the front side of the box was used. Animals had to reach the palatable food pellet (20 mg dustless precision sucrose-flavored food pellets (Bio Serv) from a shelf (4 cm wide × 8 cm long) in front of the vertical slit. Mice were habituated to the sucrose-flavored pellets for 3 consecutive days before the tests, which consisted of three phases: habituation, unskilled reaching, and skilled reaching. In the habituation phase (two sessions), mice were placed in the testing cage and 10 pellets were scattered on the floor. The session finished when mice had eaten all the pellets or 10 min had passed. For the unskilled reaching test, food pellets were placed one by one on the shelf within the mouse's tongue-reaching distance. The test finished when 10 pellets were eaten or 4 min had passed. In the skilled reaching test, food pellets were placed one by one on the shelf 1.5 cm away from the slit, so that mice had to use their forelimbs to reach them. Pellet grasping and retrieval was scored as a success, and pellet displacement without retrieval was scored as an error. The test finished within 6 min. Results are represented as percentage of success [(total successes/total trials) × 100]. The absence of phenotypic alterations in $CB_1^{-/-}$ and *Nex–*$CB_1^{-/-}$ mice in the unskilled task was used as a control that CB_1 receptor ablation per se does not interfere with the test by influencing factors different from corticospinal function. Complementary analysis of motor impairment in $CB_1^{-/-}$ mice was conducted by using the staircase reaching test (Campden Instruments). This test allows measurement of coordinated paw reaching in rodents. The system is formed by two stairs with eight steps each on which two rewarding food pellets can be placed. The test consisted of three phases: training, unskilled reaching, and skilled reaching. Habituation to sucrose-flavored food pellets was performed for 3 consecutive days, and then mice were habituated to the apparatus for 2 d by placing some pellets along the central corridor and stairs. On 5 consecutive training days, both stairs were filled with two pellets per stair, and mice were challenged to reach pellets that had been placed exclusively in the stairs for 10 min. In two additional test sessions, animals were challenged to reach pellets placed in the five lowest steps, which need the use of a paw to be reached (note that the three upper steps can be reached with the tongue and thus are not useful to assess paw skilled reaching ability). Finally, the patch removal test was conducted to measure skilled motor performance by assessing the ability of the mouse to remove a piece of adhesive patch placed in each hindpaw as described previously (Tomassy et al., 2010). Adhesive patches were placed in each hindpaw of the mouse, and the animal was placed in a normal housing cage and video recorded. The test finished when both patches had been removed or 4 min had passed. The time of latency for the first nose contact with the patch was determined, thus providing a general assessment of the sensorial status. Skilled patch removal ability was measured by calculating the mean number of contacts until each adhesive patch had been removed. Results shown correspond to the average of two tests. Additional characterization of general motor activity, exploration, and coordination was performed in ActiTrack and RotaRod devices as described previously (Blazquez et al., 2011).

DiI labeling. Labeling of corticospinal tracts with the lipophilic carbocyanine dye DiI (1,1′-diotadecyl-3,3,3′,3′-tetramethylindocarbocyanine; Invitrogen) was performed in the brains of *Nex–*$CB_1^{-/-}$ and $CB_1^{f/f}$ mice at P2. A single crystal of DiI was picked up on a fire-polished tip of a broken glass micropipette and inserted into the presumptive motor cortex. The DiI-containing brains were incubated in PBS/0.1% sodium azide at 50°C in the dark for 4 weeks. Brains embedded in 3% agar were sectioned at 100 μm in the sagittal plane, counterstained with DAPI, and mounted with PBS. Axon projections were visualized using a Carl Zeiss AxioImager M1 with 5× magnification and 0.16 numerical aperture Zeiss objectives. Confocal images were obtained using a Carl Zeiss 510 system with 10×/0.45 numerical aperture (air) objective lens.

Data analyses and statistics. Results shown represent the means ± SEM, and the number of experiments is indicated in every case. Statistical analysis was performed by one- or two-way ANOVA, as appropriate. A *post hoc* analysis was made by the Student–Neuman–Keuls test.

Results

The CB_1 cannabinoid receptor regulates cortical layer neuron specification

We initially determined the impact of CB_1 receptor inactivation on cortical development by analyzing cortical thickness of $CB_1^{-/-}$ and WT littermates. $CB_1^{-/-}$ mice showed enlarged ventricles at P2, in agreement with the described alterations induced by *in utero* CB_1 receptor pharmacological blockade (Mulder et al., 2008). A reduction of total cortical thickness was evident at P2 in $CB_1^{-/-}$ mice (total cortical thickness, 527 ± 26 μm in WT mice vs 475 ± 15 μm in $CB_1^{-/-}$ mice; $p < 0.05$), which was attributable to deep-layer but not upper-layer thickness reduction (upper- and deep-layer cortical thickness, 174 ± 26 and 352 ± 28 μm in WT mice vs 172 ± 5 and 302 ± 20 μm in $CB_1^{-/-}$ mice; $p < 0.05$ for deep-layer cortical thickness; $n = 6$ for each group). These results support a significant role of the CB_1 receptor in controlling progenitor population size and raise the question of whether CB_1 receptor signaling exerts a selective function in the differentiation of the neuronal populations of the different cortical layers. Because Tbr1 is an early expressed T-box transcription factor that promotes deep-layer specification and corticothalamic neuron projections (Hevner et al., 2001; Han et al., 2011), we first analyzed postmitotic $Tbr1^+$ neuroblasts along the developing cortex in CB_1 receptor-deficient mice. Quantification of $Tbr1^+$ cells in equal-sized bins at E16.5 showed that these postmitotic cells accumulated abnormally in deep bins of the cortical plate of $CB_1^{-/-}$ mice compared with WT littermates (Fig. 1*A*, middle column, *B*). Moreover, the distribution of neurons that express the upper-layer neuronal marker Satb2 was also affected (Fig. 1*A*, right column), and, in particular, $Satb2^+$ cells were expanded in the lower bins 2–3 (Fig. 1*C*). Double marker analysis further showed that CB_1 receptor deletion increased the number of cells that coexpress Tbr1 and Satb2 (Fig. 1*D*,*E*). Satb2 is a well-known repressor of Ctip2, a selective layer 5b marker of subcerebral projection neurons, and this repressive action of Satb2 promotes callosal projection-neuron identity (Alcamo et al., 2008). We sought to investigate the impact of CB_1 deletion in the development of $Satb2^+$ and $Ctip2^+$ neuronal cell populations. $Satb2^+$ cells in $CB_1^{-/-}$ cortices at E16.5 were intermingled among $Ctip2^+$ cells, and an increased number of cells coexpressing both markers were evident during CB_1 receptor inactivation (Fig. 1*D*,*F*). $Satb2^+$ cell number in the total cortical column was significantly increased (Fig. 1*G*), and consequently $Ctip2^+$ cells were reduced in $CB_1^{-/-}$ mice compared with WT littermates (Fig. 1*H*).

Considering the altered expression of neuronal specification markers induced by genetic ablation of CB_1, we performed gene expression analysis of selected transcription factors involved in the regulation of corticogenesis in E14.5 cortical extracts. CB_1 receptor inactivation impaired the expression of determinants known to be involved in fate specification and development of deep- and upper-layer cortical neurons. Thus, CB_1 receptor deficiency decreased the expression of the deep-layer neuronal markers Fezf2 and Ctip2 (relative mRNA levels, 0.55 ± 0.07 vs 1.00 ± 0.15 in WT cortices and 0.47 ± 0.06 vs 1.00 ± 0.13 in WT

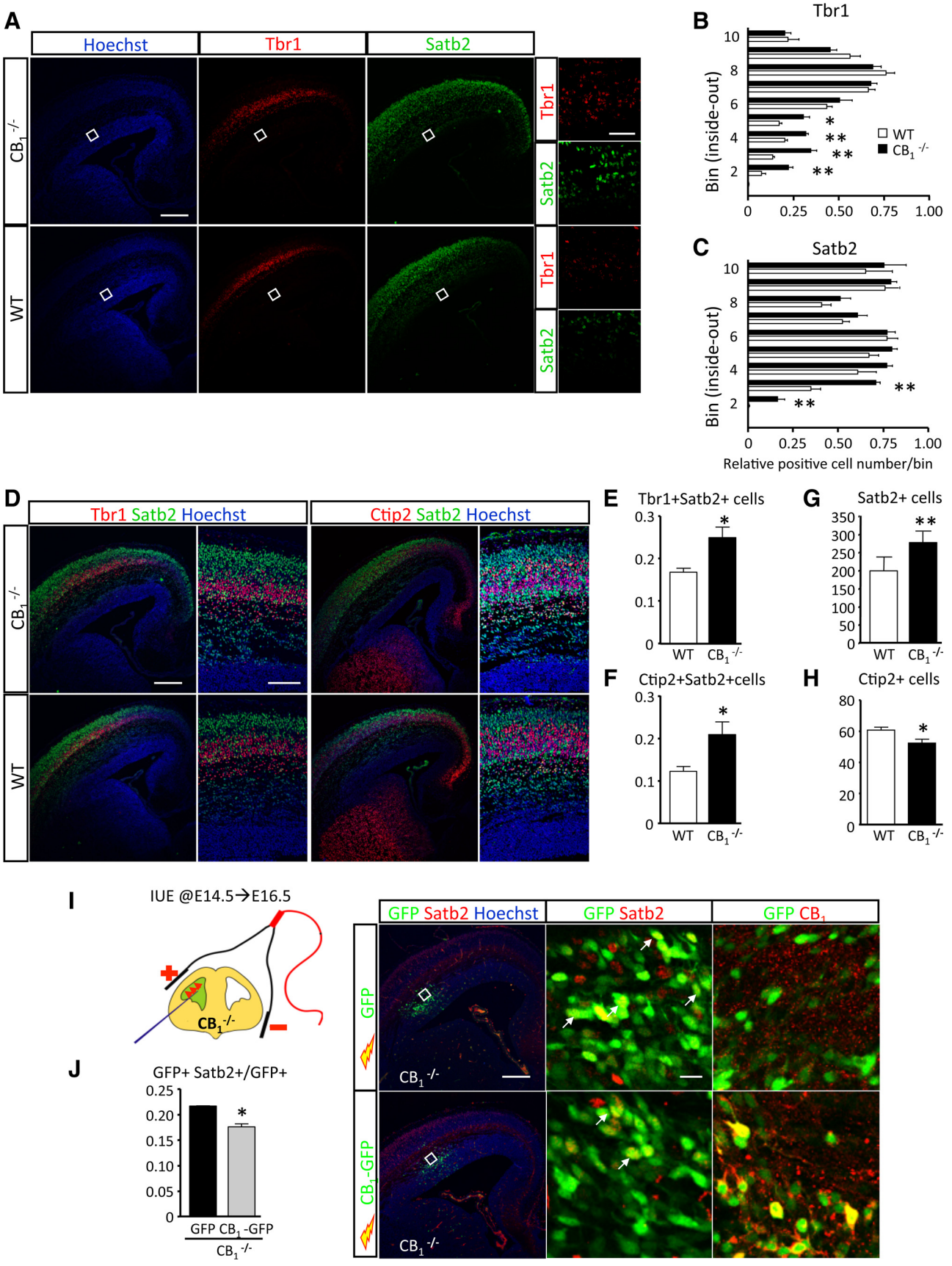

Figure 1. CB_1 receptor inactivation interferes with the specification of upper- and deep-layer cortical neurons. ***A***, $CB_1^{-/-}$ mice and WT littermates were analyzed at E16.5, and Tbr1$^+$ and Satb2$^+$ cells were revealed by immunofluorescence. Low- and high-magnification representative images are shown. ***B***, ***C***, The fraction of differentiating cells that express Tbr1 and Satb2 in $CB_1^{-/-}$ and WT mice (black and white bars, respectively) was quantified in equal-size binned areas and referred to total cell number (Hoechst 33528 counterstaining). ***D***, Immunofluorescence analysis was performed in WT and $CB_1^{-/-}$ mice at E16.5 for Tbr1$^+$, Ctip2$^+$, and Satb2$^+$ cells. Representative images of Tbr1–Satb2 and Ctip2–Satb2 immunoreactivity are shown (*Figure legend continues.*)

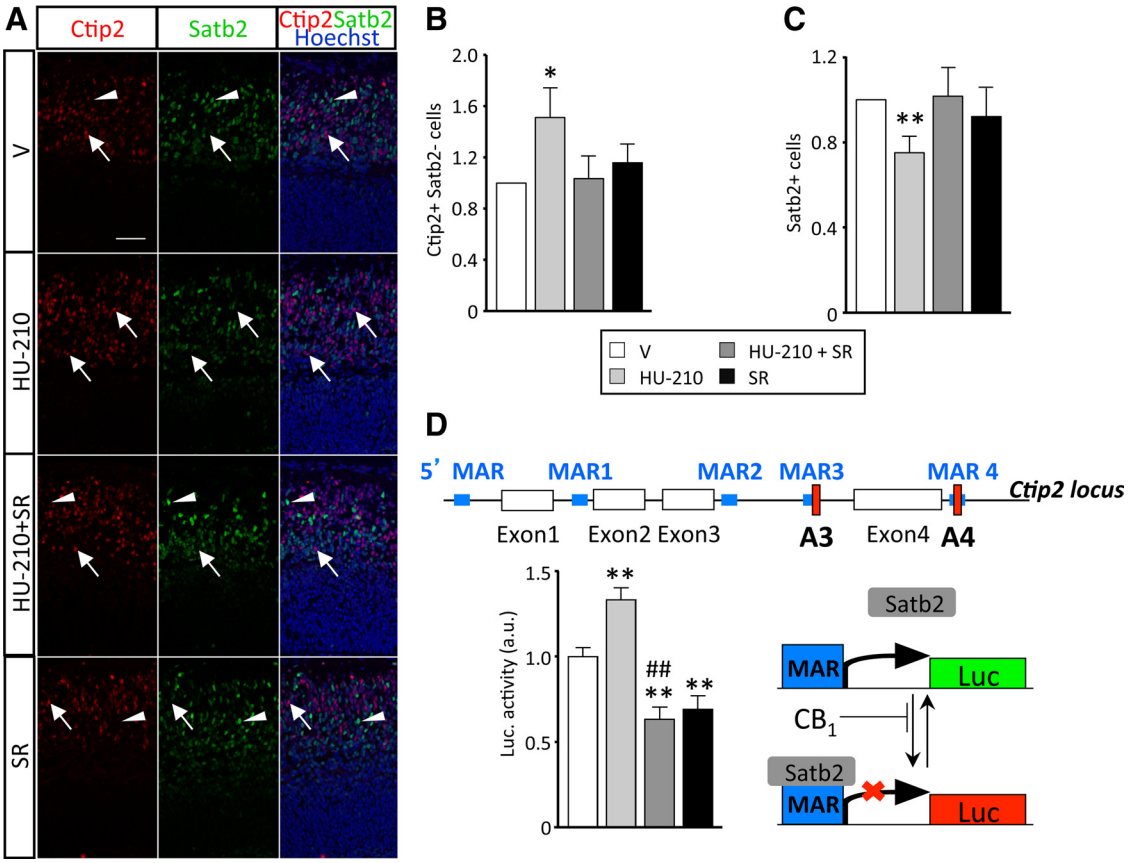

Figure 2. CB_1 receptor signaling promotes Ctip2$^+$ neuron differentiation. ***A***, Cortical organotypic cultures form E13.5 WT embryos were treated for 3 d with vehicle (V) or HU-210 (5 μM), alone or combined with SR141716 (25 μM). Representative immunofluorescence images of Ctip2$^+$ and Satb2$^+$ cells are shown (red and green, respectively). ***B***, ***C***, The fraction of Ctip2-only positive cells (arrows) and Satb2$^+$ cells (arrowheads) were quantified in the same conditions and referred to total cell number (Hoechst 33528 counterstaining). Results correspond to four independent experiments. ***D***, HiB5 neural stem cells were transfected with a luciferase reporter construct that contained the A4 MAR sequence of the Ctip2 locus together with pCAG–CB_1 and pMSCV–Satb2. Ctip2-luciferase activity was determined 36 h after treatment with vehicle (V) or HU-210 (50 nM), alone or combined with SR141716 (1 μM). *$p < 0.05$, **$p < 0.01$ versus vehicle-treated cells; ##$p < 0.01$ versus HU-210-treated cells. Scale bar: ***A***, 50 μm.

cortices; $p < 0.05$ and $p < 0.01$, respectively; $n = 4$ for each group) (Arlotta et al., 2005; Chen et al., 2008) and the corticofugal neuronal marker Sox5 (relative mRNA levels, 0.50 ± 0.05 vs 1.00 ± 0.11 in WT cortices; $p < 0.05$) (Lai et al., 2008). Conversely, levels of the upper-layer transcription factor Satb2 were upregulated in $CB_1^{-/-}$ cortices (relative mRNA levels, 2.65 ± 0.15 vs 1.00 ± 0.23 in WT cortices; $p < 0.05$). To validate the role of the CB_1 receptor in the correct expression of upper/deep-layer neuronal specification markers, we performed a gain-of-function strategy aimed at rescuing CB_1 receptor expression in a $CB_1^{-/-}$ background by *in utero* electroporation of a pCAG–CB_1–GFP expression vector (Fig. 1*I*). Importantly, reexpression of the CB_1 receptor reduced the expansion of Satb2$^+$ cells that occurred in deep bins of $CB_1^{-/-}$ cortices and thus reduced the number of GFP$^+$Satb2$^+$ cells (Fig. 1*I*, arrows, *J*).

The CB_1 cannabinoid receptor controls deep-layer neuron specification through the regulation of Ctip2–Satb2 balance

We further evaluated the role of the CB_1 receptor in the regulation of deep-layer neuronal specification by analyzing the changes in the Ctip2–Satb2 axis in cortical organotypic cultures of E13.5 WT mice. Treatment with HU-210, a CB_1 receptor synthetic agonist, increased the number of Ctip2-only positive cells but decreased the number of Satb2$^+$ cells (Fig. 2*A–C*, arrows and arrowheads, respectively). The induction of neuronal differentiation to Ctip2$^+$ cells by HU-210 and its inhibitory effect on Satb2$^+$ cell differentiation were prevented by the CB_1 receptor-selective antagonist SR141716 [*N*-piperidino-5-(4-chlorophenyl)-1-(2,4-dichlorophenyl)-4-methyl-3-pyrazole carboxamide]. Because Satb2 negatively regulates Ctip2 expression by binding to MAR sequences at the Ctip2 promoter (Alcamo et al., 2008; Britanova et al., 2008), we performed luciferase reporter assays for different MAR regions of the Ctip2 promoter in the HiB5 neural stem cell line. HiB5 cells were transiently transfected with luciferase constructs under the control of the Satb2-binding sites A4 or A3 of the Ctip2 promoter together with expression vectors for CB_1 and Satb2. HU-210 treatment increased A4–fosluc activity (Fig. 2*D*), and this effect was prevented by CB_1 receptor blockade with SR141716. Likewise, HU-210 increased A3–fosluc activity (data not

←

(*Figure legend continued.*) (left and right panels, respectively). ***E***, ***F***, Quantification of the neuronal cell fraction that coexpress Tbr1 with Satb2 and Satb2 with Ctip2, respectively, referred to total cell number (Hoechst 33528 counterstaining) in the cortical column of WT and $CB_1^{-/-}$ mice (white and black columns, respectively). ***G***, ***H***, Satb2$^+$ and Ctip2$^+$ cells were quantified in 50-μm-wide cortical columns of the same mice. ***I***, ***J***, *In utero* electroporation (IUE) of E14.5 $CB_1^{-/-}$ mice was performed with pCAG–GFP vector and pCAG–CB_1–GFP to reexpress CB_1 receptor (black and gray bars, respectively), and cortices were subsequently analyzed at E16.5. Satb2$^+$ cells in the GFP$^+$ electroporated cell population were quantified. Arrows indicate electroporated double GFP$^+$Satb2$^+$ cells. $n = 5$ for each group in ***A–G*** and $n = 2$ for each group in ***H*** and ***I***. Scale bars: ***A***, 250 μm and inset, 35 μm; ***D***, 250 and 100 μm; ***I***, 250 μm and inset, 20 μm. *$p < 0.05$, **$p < 0.01$ versus control mice.

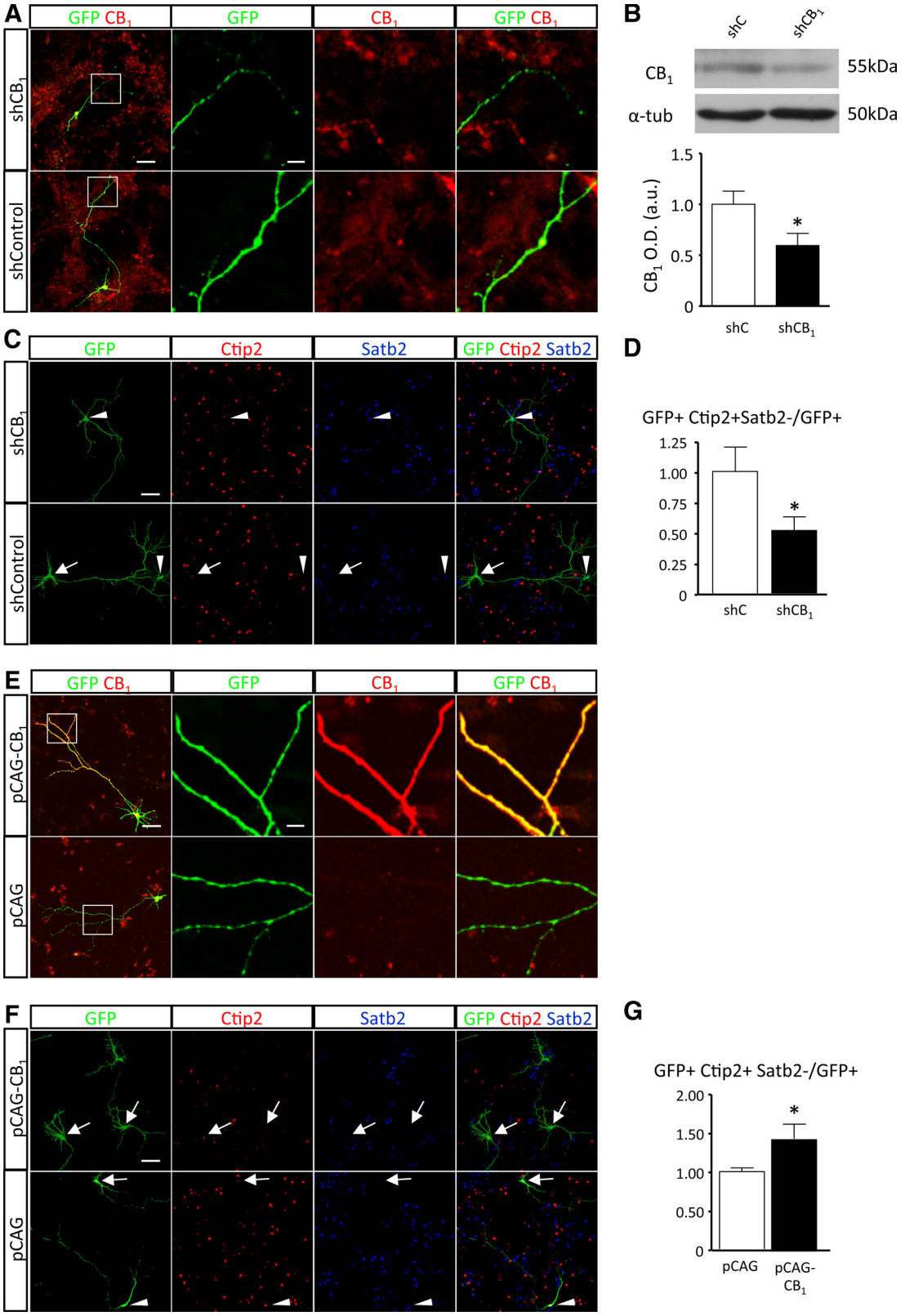

Figure 3. Manipulation of CB_1 receptor expression controls Ctip2$^+$ neuron differentiation. ***A***, Primary cortical cultures obtained from E13.5 WT cortices after *ex utero* electroporation with shControl and $shCB_1$ were allowed to differentiate for 7 d *in vitro* (DIV). Low- and high-magnification images are shown of CB_1 receptor expression (red) in electroporated cells identified with GFP antibody (green). ***B***, Western blot analysis of CB_1 receptor knockdown after transfection of shControl (shC) and $shCB_1$ in P19 cells. α-tub, α-Tubulin; O.D., optical density; a.u., arbitrary units. ***C***, ***D***, Ctip2-only-positive cells (arrow) and Satb2$^+$ cells (arrowheads) were quantified in the electroporated GFP$^+$ cell subpopulation. Representative immunofluorescence images are shown. ***E***, Primary cortical cultures of E13.5 WT cortices after *ex utero* electroporation with pCAG and pCAG–CB_1 and differentiation 7 DIV. Low- and high-magnification images are shown of CB_1 receptor expression in electroporated cells identified with GFP antibody. ***F***, ***G***, Ctip2-only-positive cells (arrows) and Satb2$^+$ cells (arrowhead) were quantified in the electroporated GFP$^+$ cell subpopulation. Representative immunofluorescence images are shown. Scale bars: ***A***, 50 and 10 μm; ***C***, ***F***, 50 μm; ***E***, 50 and 10 μm. *$p < 0.05$ versus control-electroporated cells. Results correspond to four independent experiments.

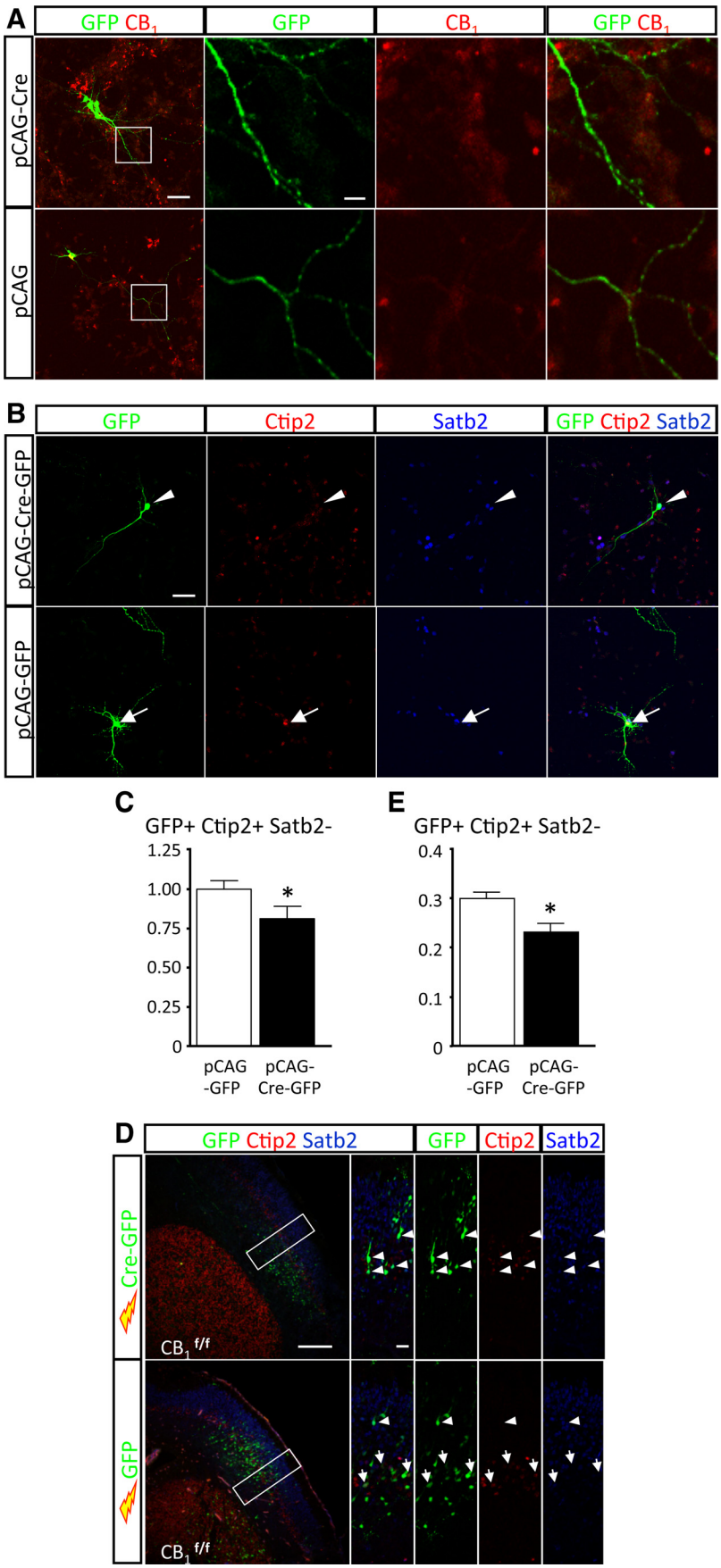

Figure 4. ***A***, CB_1 receptor expression was analyzed in electroporated cells (GFP^+) in $CB_1^{f/f}$-derived cells after pCAG–GFP or pCAG–CRE–GFP electroporation of $CB_1^{f/f}$ cortices. ***B***, ***C***, Ctip2-only-positive cells (arrow) and $Satb2^+$ cells (arrowhead) were quantified in the electroporated GFP^+ cell subpopulation. Representative immunofluorescence images are shown. Results correspond to four independent experiments. ***D***, ***E***, *In utero* electroporation of E12.5 $CB_1^{f/f}$ mice was performed with pCAG–GFP and pCAG–CRE–GFP vectors, and pups were subsequently analyzed at P0. Ctip2-only-positive cells that were electroporated ($Ctip2^+Satb2^-GFP^+$) were quantified, and the relative number to the GFP^+ cell population is shown. Arrows indicate electroporated $Ctip2^+Satb2^-GFP^+$ cells (arrowheads indicate $Satb2^+GFP^+$ cells). $n = 3$ for each group. $^*p < 0.05$ versus control electroporated cells or pups. Scale bars: ***A***, 50 and 10 μm; ***B***, 50 μm; ***D***, 250 and 25 μm.

shown). Thus, CB_1 receptor activity prevents the repressive effect of Satb2 on the Ctip2 promoter, thereby increasing its activity.

To directly assess the role of the CB_1 receptor in deep-layer neuronal differentiation, we electroporated E13.5 mouse cortices, when CSMN generation is maximal (Tomassy et al., 2010), with a GFP^+ vector, and the CB_1 receptor was knocked down or overexpressed with $shCB_1$ and pCAG–CB_1, respectively. Cortical cultures were obtained by dissociation and allowed to differentiate for 7 d *in vitro*. Efficient manipulation of CB_1 receptor expression under these conditions was evaluated by CB_1 and GFP immunofluorescence (Fig. 3*A*,*E*). In addition, we validated the effect of $shCB_1$ by Western blot analysis (Fig. 3*B*) and real-time PCR. $shCB_1$ reduced CB_1 protein and mRNA levels when compared with shControl (relative CB_1 protein levels in shControl and $shCB_1$, 1.00 ± 0.13 and 0.59 ± 0.15, $p < 0.01$; relative CB_1 mRNA levels in shControl and $shCB_1$, 1.00 ± 0.23 and 0.46 ± 0.17, $p < 0.01$). Immunofluorescence characterization of neuronal populations among the electroporated GFP^+ population after differentiation revealed that CB_1 receptor downregulation decreased the generation of Ctip2-only-positive cells (Fig. 3*C*,*D*), whereas CB_1 receptor overexpression increased $Ctip2^+$ cells (Fig. 3*F*,*G*). In addition, CB_1 ablation by *ex utero* electroporation of pregnant E13.5 $CB_1^{f/f}$ brains was conducted with a Cre recombinase expression vector (Fig. 4*A*). Using this strategy to achieve acute CB_1 receptor loss of function, we also observed reduced $Ctip2^+$ differentiation of cortical cells when compared with GFP^+ cells (Fig. 4*B*, arrows, *C*). To further validate the results derived from *ex utero* CB_1 receptor manipulation, we performed *in vivo in utero* electroporation with the pCAG–Cre–GFP and pCAG–GFP plasmids, and pups were analyzed at P0 (Fig. 4*D*). Noteworthy, *in*

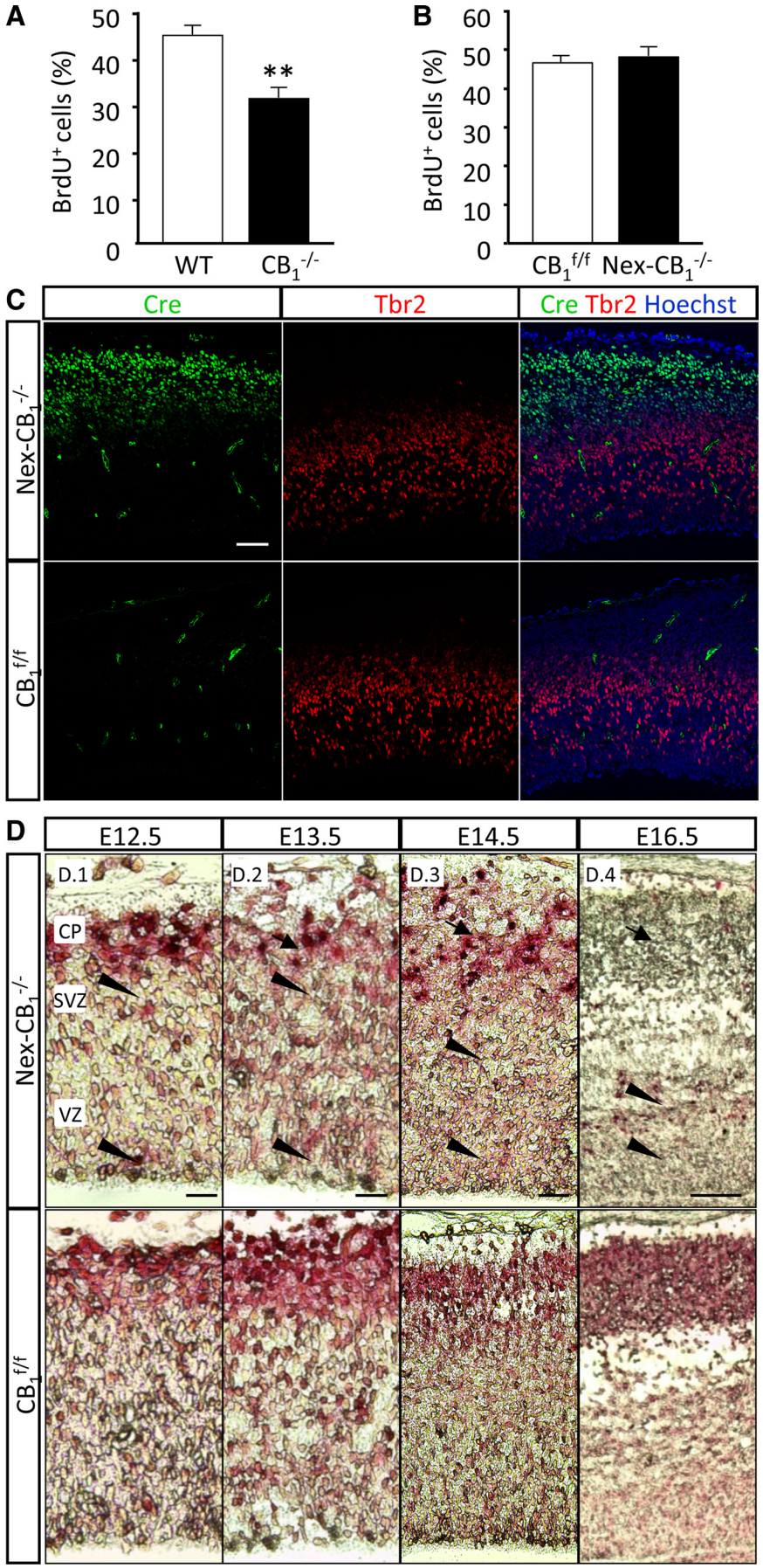

Figure 5. Cortical progenitor cell proliferation is not affected in conditional *Nex–$CB_1^{-/-}$* mice. ***A***, ***B***, Quantification of progenitor cell proliferation as BrdU-labeled cells in the VZ/SVZ of *$CB_1^{-/-}$* mice and WT littermates, and *Nex–$CB_1^{-/-}$* mice and *$CB_1^{f/f}$* littermates, at E14.5. ***C***, Cre recombinase expression in the same animals as determined by immunofluorescence analysis of Cre and Tbr2 (green and red, respectively). ***D***, *In situ* hybridization of CB_1 mRNA in *Nex–$CB_1^{-/-}$* mice and *$CB_1^{f/f}$* littermates at E12.5, E13.5, E14.5, and E16.5 (***D.1–D.4***, respectively). Arrows indicate CB1 mRNA reduced expression in postmitotic cortical areas; arrowheads indicate preserved expression in VZ/SVZ. Scale bars: ***C***, ***D.3***, 50 μm; ***D.1***, ***D.2***, 30 μm; ***D.4***, 100 μm.

utero CB_1 receptor ablation decreased Ctip2$^+$ neuronal differentiation when compared with control *$CB_1^{f/f}$* cortices (Fig. 4*E*). These results support that CB_1 receptor activity is required for the appropriate expression of the deep-layer neuronal determinant Ctip2.

The CB_1 cannabinoid receptor independently regulates progenitor proliferation and neuronal differentiation

Because CB_1 receptor loss of function is ensued by alterations in neuronal specification during cortical development (present study) and the CB_1 receptor is also known to be expressed in progenitor cells, on which it drives VZ/SVZ progenitor proliferation in a cell-autonomous manner (Aguado et al., 2005; Mulder et al., 2008), a plausible hypothesis would be that CB_1-receptor-mediated regulation of neuronal specification was a direct consequence of its role on progenitor generation. To investigate the putative relationship between changes in cortical progenitor proliferation and neuronal specification, we next compared complete *$CB_1^{-/-}$* mutant mice and glutamatergic-specific *Nex–$CB_1^{-/-}$* mutant mice. In the latter mutants, CB_1 is selectively deleted in glutamatergic neurons of the dorsal telencephalon (Monory et al., 2006). Cre recombinase expression under the control of the Nex regulatory sequences was described to selectively target neurons of the developing cortex rather than cortical progenitors (Wu et al., 2005). However, the impact of conditional *Nex–$CB_1^{-/-}$* deletion during cortical development is unknown. Complete *$CB_1^{-/-}$* mice showed reduced progenitor proliferation in the developing cortex (Aguado et al., 2005), whereas no differences in progenitor cell proliferation were evident between *$CB_1^{f/f}$* and *Nex–$CB_1^{-/-}$* mice (Fig. 5*A*,*B*). Immunofluorescence analysis showed that Cre expression at E14.5 occurred in postmitotic areas of the developing cortex beyond the basal edge of the SVZ, as identified by the expression pattern of its marker Tbr2 (Fig. 5*C*). *In situ* hy-

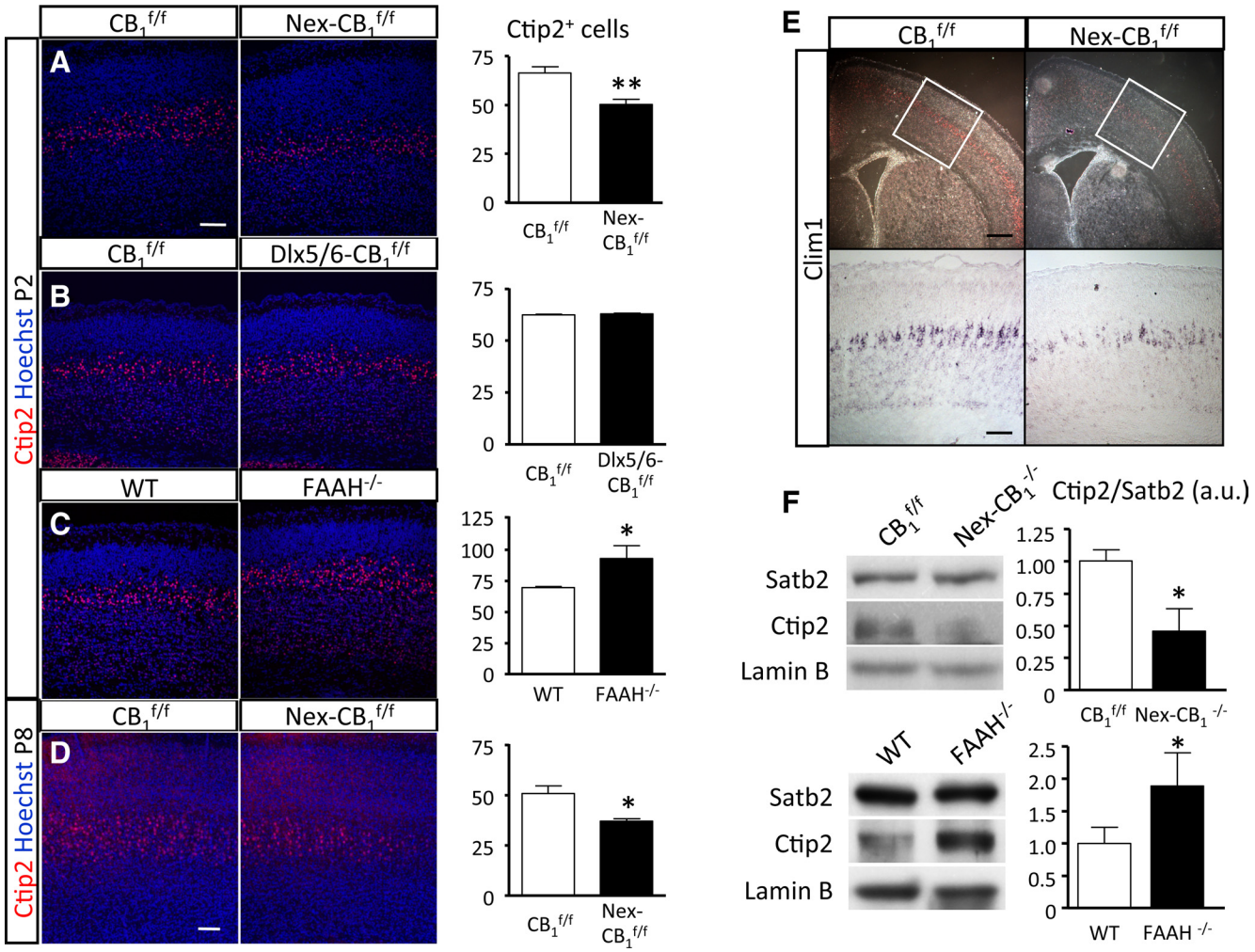

Figure 6. CB_1 receptor signaling regulates the generation of deep-layer Ctip2$^+$ neurons. ***A–D***, *Nex–$CB_1^{-/-}$*, *Dlx5/6–$CB_1^{-/-}$*, and *$FAAH^{-/-}$* mice and their respective wild-type (*$CB_1^{f/f}$* and WT) littermates were analyzed at P2, and Ctip2$^+$ neurons were quantified in 50-μm-wide cortical columns ($n = 8$ and 9, 2 and 3, and 2 and 3, respectively, for each group). *Nex–$CB_1^{-/-}$* and WT littermates were also analyzed at P8 (***D***; $n = 4$ for each group). Representative images are shown (left). ***E***, *In situ* hybridization of Clim1 at P2 in *$CB_1^{f/f}$* and *Nex–$CB_1^{-/-}$*. ***F***, Western blot analyses of nuclear extracts obtained from P2 cortices of *Nex–$CB_1^{-/-}$* and *$FAAH^{-/-}$* mice compared with their corresponding WT littermates. The relative protein levels of Ctip2 and Satb2 were quantified after densitometry, and loading control was performed with anti-lamin B1 antibody. a.u., Arbitrary units. Scale bars: ***A***, 50 μm; ***D***, 150 μm; ***E***, 150 (top) and 50 (bottom) μm.* $p < 0.05$, ** $p < 0.01$ versus WT mice sections.

bridization experiments at different stages demonstrated that *Nex–$CB_1^{-/-}$* mice preserved CB_1 expression at early proliferative stages in VZ/SVZ cells and only postmitotic neuroblasts lost their expression (Fig. 5*D*). In agreement with the notion that the CB_1 receptor regulates neuronal differentiation independently of its actions on the progenitor cell pool, the observed increase in Satb2$^+$ cells in *$CB_1^{-/-}$* was not attributable to its aberrant expression in apical or basal progenitor cells (data not shown). These findings demonstrated that the combined use of conditional *Nex–$CB_1^{-/-}$* and complete *$CB_1^{-/-}$* mice allows discriminating between CB_1 receptor actions in VZ/SVZ neural progenitor populations and CB_1-receptor-mediated regulation of differentiating postmitotic neuronal cells.

Deficient development of deep-layer Ctip2$^+$ neurons in the absence of the CB_1 cannabinoid receptor

To avoid the possible confounding interactions with impaired progenitor proliferation that occur in *$CB_1^{-/-}$* mice, we therefore turned to investigate the development of deep-layer Ctip2$^+$ neurons in *Nex–$CB_1^{-/-}$* mice. The number of Ctip2$^+$ cells at P2 along the cortical plate was reduced in *Nex–$CB_1^{-/-}$* mice compared with their WT littermates (Fig. 6*A*). Of importance, this effect was still evident at P8 (Fig. 6*D*). The direct regulatory action of CB_1 receptor in the specification of the pyramidal lineage was confirmed by analyzing *Dlx5/6–$CB_1^{-/-}$* mice, which lack CB_1 in GABAergic neurons of the forebrain (Monory et al., 2006). CB_1 receptor deletion in the GABAergic lineage did not interfere with the generation of Ctip2$^+$ cells (Fig. 6*B*). Substantiating a putative regulatory action of the eCB tone in cortical layer specification, mice deficient in fatty acid amide hydrolase (FAAH), a major eCB-degrading enzyme, showed an increased number of Ctip2$^+$ cells and, therefore, an opposite phenotype to *Nex–$CB_1^{-/-}$* mice (Fig. 6*C*). In addition, *in situ* hybridization for Clim1 (Ldb2), a transcription factor that labels subcerebral projection neurons of layer 5 (Azim et al., 2009), revealed a severe reduction of Clim1$^+$ neurons in *Nex–$CB_1^{-/-}$* mice (Fig. 6*E*). Furthermore, Western blot analysis of nuclear extracts from *Nex–$CB_1^{-/-}$* cortices showed reduced Ctip2 protein levels relative to Satb2 expression, whereas the opposite was observed in *$FAAH^{-/-}$* cortical extracts (Fig. 6*F*).

The CB_1 cannabinoid receptor regulates subcerebral projection neuron development

The alterations induced by CB_1 receptor inactivation in the proneurogenic layer specification program prompted us to investi-

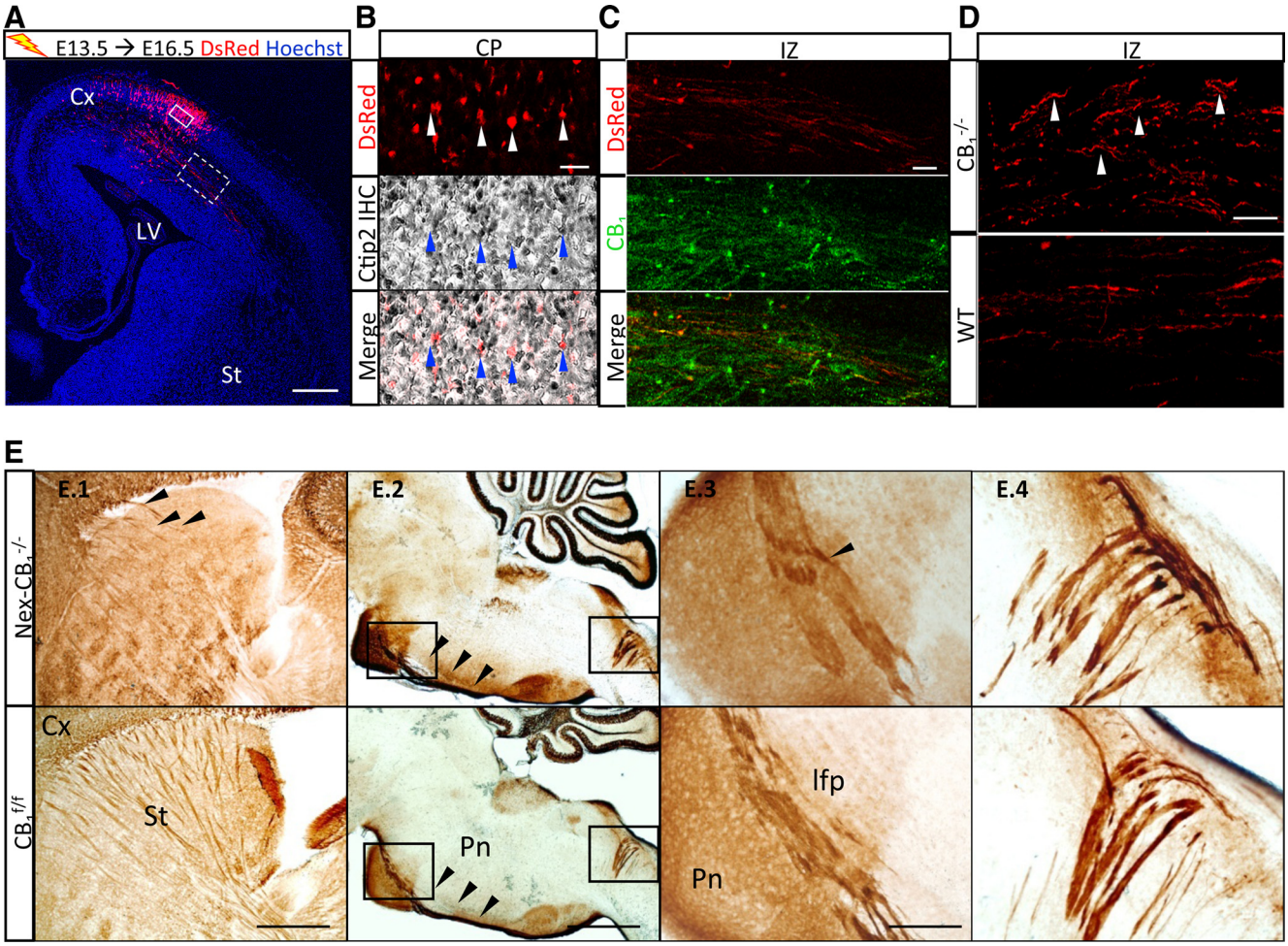

Figure 7. CB_1 receptor signaling controls axon navigation of CSMNs. $CB_1^{-/-}$ mice and WT littermates were electroporated *in utero* at E13.5 with pCAG–DsRed and fluorescence analysis was performed 3 d later. ***A***, Low-magnification image indicating the position of the analyzed insets (***B***, ***C***, solid and dashed lines, respectively). ***B***, $DsRed^+$ somata in the cortical plate show colocalization with Ctip2 immunoreactivity (middle and bottom). ***C***, Representative image of $DsRed^+$ axons expressing CB_1 receptors in the IZ of WT mice. ***D***, Navigating $DsRed^+$ axons in the IZ of WT and $CB_1^{-/-}$ mice (arrowheads). Representative images of each genotype are shown ($n = 3$). ***E***, PKCγ immunostaining images in sagittal brain sections of *Nex–*$CB_1^{-/-}$ and $CB_1^{f/f}$ mice at P8 ($n = 4$ for each group). Aberrant axonal trajectories (arrowheads) were found in corticospinal tracts in the corticostriatal junction (***E.1***). The corticospinal tract is defined in the hindbrain of *Nex–*$CB_1^{-/-}$ and control mice (***E.2***, arrowheads), but aberrant axonal fasciculation was detected in corticospinal tracts of *Nex–*$CB_1^{-/-}$ animals as they traverse the pons (***E.3***) and reach the spinal cord (***E.4***). CC, Corpus callosum; Cx, cortex; lfp, longitudinal fasciculus of the pons; LV, lateral ventricle; CP, cortical plate; Pn, pons; St, striatum. Scale bars: ***A***, ***E.3***, ***E.4***, 200 μm; ***B***, ***C***, 50 μm; ***D***, 25 μm; ***E.1***, 500 μm; ***E.2***, 1 mm.

gate its impact on axonal projection and connectivity. In line with previous observations (Mulder et al., 2008; Wu et al., 2010), aberrant corticofugal projections were found upon CB_1 deletion. Immunofluorescence microscopy analysis of the L1 neural cell adhesion molecule revealed subcortical projection deficits in P2 $CB_1^{-/-}$ and *Nex–*$CB_1^{-/-}$ mice but not in *Dlx5/6–*$CB_1^{-/-}$ mice (data not shown). The corticostriatal boundary of *Nex–*$CB_1^{-/-}$ mice showed altered axonal trajectories, and, in the intermediate zone (IZ), disorganized and enlarged fascicles were evident (data not shown). These results, together with the involvement of the CB_1 receptor in the differentiation of deep-layer $Ctip2^+$ neurons, from where corticospinal projections arise (Molyneaux et al., 2007), prompted us to investigate the role of the CB_1 receptor in subcerebral axonal projections. We performed *in utero* electroporation experiments with pCAG–DsRed in $CB_1^{-/-}$ mice at E13.5 and analyzed $DsRed^+$ projections at E16.5 (Fig. 7*A*). The corticospinal nature of DsRed-labeled axons was confirmed by the $Ctip2^+$ immunoreactivity shown by $DsRed^+$ somata (Fig. 7*B*). In WT embryos, labeled projecting axons expressed CB_1 receptor (Fig. 7*C*) and showed straight trajectories, whereas profound alterations of navigating $DsRed^+$ axons were observed at the IZ of CB_1-deficient mice (Fig. 7*D*). To confirm more precisely the exact nature of these subcortical projection alterations, we performed immunohistochemical analysis of PKCγ, because this protein is present in corticospinal tracts. Similar to the aberrant pattern of L1 immunofluorescence, abnormal axonal trajectories of PKCγ-labeled tracts in the corticostriatal junction were evident at P8 in *Nex–*$CB_1^{-/-}$ mice compared with WT littermates (Fig. 7*E.1*). Although no major alterations of the corticospinal tract in the posterior hindbrain of *Nex–*$CB_1^{-/-}$ were observed, these animals had aberrant CSMN projections as axons traverse the pons (Fig. 7*E.2*,*E.3*), those projections reaching the spinal cord in a notably less organized manner (Fig. 7*E.4*).

To unequivocally ascribe a role for the CB_1 receptor in the development of layer 5 subcerebral neurons, we took advantage of Thy1–YFP–H mice, in which the expression of the fluorescent protein under the control of the neuronal promoter of the *Thy-1* gene (encoding Thy-1 membrane glycoprotein precursor) occurs selectively in layer 5 projection neurons, thus allowing the visualization of corticospinal tracts (Feng et al., 2000; Tomassy et al.,

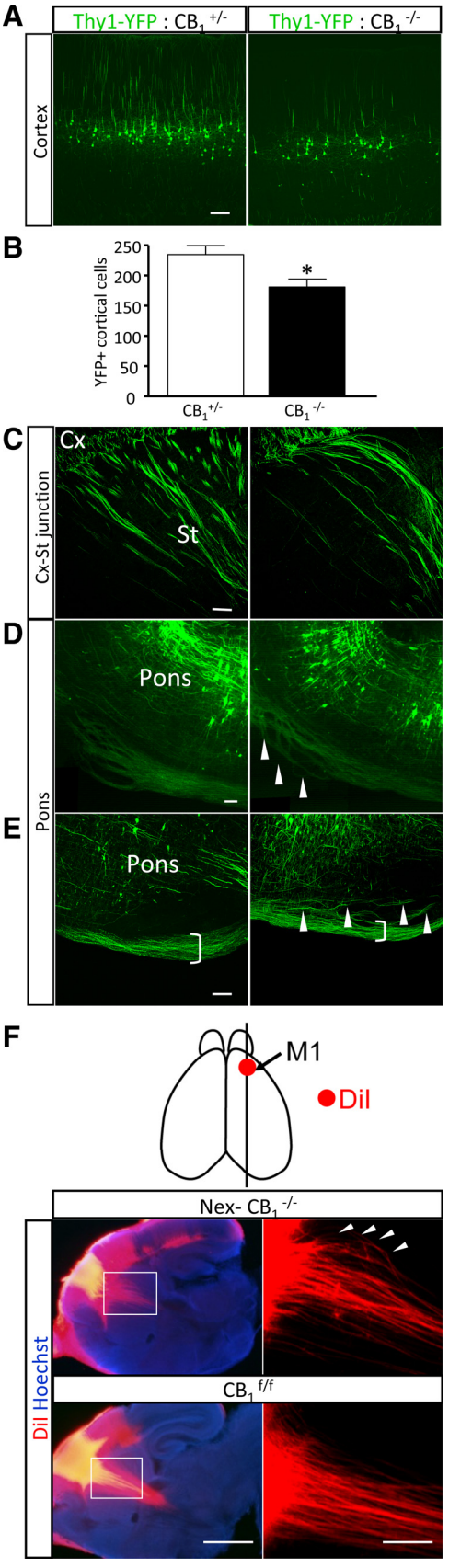

Figure 8. CB_1-deficient Thy1–YFP mice show alterations of subcerebral projection neurons. ***A***, ***B***, Confocal fluorescence images of sagittal sections of P21 cortices from *Thy1–YFP:*$CB_1^{+/-}$ and *Thy1–YFP:*$CB_1^{-/-}$ littermates. Fluorescent somata of putative CSMNs in layer 5 were quantified. $n = 2$ and 3, respectively. ***C***, ***D***, Fluorescence images illustrating corticospinal tract at the level of the corticostriatal junction and pons. ***E***, Confocal images at a more caudal level of the pons. Arrowheads indicate major alterations observed in *Thy1–YFP:*$CB_1^{-/-}$. ***F***, Projected images of DiI-labeled corticospinal tracts originating from the M1 cortex in $CB_1^{f/f}$ and *Nex–*$CB_1^{-/-}$ mice at P2. Inset shows misrouted fibers (arrowheads) found in the corticostriatal junction and traversing the striatum proximal to the cortex. Cx, Cortex; St, striatum. $^*p < 0.05$. Scale bars: ***A***, ***C***, ***E***, 150 μm; ***D***, 250 μm; ***F***, 1 mm and inset, 200 μm.

2010). We crossed $CB_1^{-/-}$ and Thy1–YFP–H mice to study the specification and development of corticospinal neurons and axonal tracts in the absence of the CB_1 receptor. At P21, a significant reduction in fluorescently labeled somata was evident in cortical layer 5 (Fig. 8*A*,*B*), whereas no changes were observed in the hippocampus (data not shown). CB_1 receptor deletion induced an aberrant phenotype of subcerebral projection neurons similar to that observed by PKC γ immunohistochemistry (Fig. 7). Thus, misrouted axons were visible while traversing the internal capsule in the corticostriatal junction in $CB_1^{-/-}$:Thy1–YFP–H mice (Fig. 8*C*), axons that reached the pons were reduced, and the remaining ones showed fasciculation alterations (Fig. 8*D*,*E*). Finally, in agreement with a role of the CB_1 receptor in subcerebral projection neuron development, anterograde DiI tracing from the motor cortex of *Nex–*$CB_1^{-/-}$ mice confirmed the existence of misrouted fibers branching off the tracts and deviating from their normal path at the corticostriatal junction (Fig. 8*F*).

The CB_1 cannabinoid receptor regulates CSMN function

The decreased Ctip2$^+$ cell population and the disruption of subcerebral axonal projections observed in $CB_1^{-/-}$ mice prompted us to investigate whether these alterations of CSMN projections result in defective cortical motor function. Evaluation of the skilled pellet-reaching task, which is dependent on CSMN-mediated connectivity (Tomassy et al., 2010), revealed that adult $CB_1^{-/-}$ mice had a remarkable impairment in fine motor function (Fig. 9*A*). The total number of trials performed during the skilled task was not significantly different between the two groups of mice, and unskilled motor activity was not affected either (Fig. 9*C*,*D*), thus indicating the selectivity of the skilled motor function deficits. Additional support for this selectivity was provided by the observation that the general motor activity, including total distance traveled, resting time, and fast movements (ActiTrack test), as well as motor coordination (RotaRod test), did not differ between $CB_1^{-/-}$ and WT mice (Fig. 10*A*). Moreover, and in concert with the neuroanatomical findings described above, the deficits in skilled motor activity observed in $CB_1^{-/-}$ mice were recapitulated in *Nex–*$CB_1^{-/-}$ mice (Fig. 9*B*).

Additional validation of the abnormal skilled motor function phenotype found in $CB_1^{-/-}$ animals was obtained by using the staircase test, which also reflects fine motor activity and is useful to evaluate motor impairment after cortical lesions (Brooks and Dunnett, 2009). $CB_1^{-/-}$ and *Nex–*$CB_1^{-/-}$ mice had a lower performance than their respective WT littermates in their ability to grasp the most difficult food pellets (steps 4–8) (Fig. 9*E–G*). Moreover, we observed that retrieval of non-challenging pellets in the staircase test (steps 1–3) was not different among genotypes (Fig. 9*H*), thus confirming the selective impairment of fine motor activity. Finally, the patch-removal task, which also evaluates sensorimotor function, was also used. *Nex–*$CB_1^{-/-}$ mice were significantly less efficient than their WT littermates in removing a piece of adhesive tape from their hindpaws, as demonstrated by the higher number of contacts required for patch removal (Fig. 10*B*, left). This decreased performance of *Nex–*$CB_1^{-/-}$ mice in patch removal reflected a fine motor function impairment rather

←

than an altered perception of the patch, as indicated by the quantification of the latency time for the first attempt to remove the patch and the total time spent removing the patch, which were not significantly different between both genotypes (Fig. 10*B*, middle and right).

Discussion

Recent studies have shown that the CB_1 receptor regulates neural progenitor proliferation and axonal navigation, thus suggesting an instructive role of the eCB system in nervous system development (Harkany et al., 2007). The present study provides new insights into the developmental role of the CB_1 receptor, revealing that it exerts a pivotal role in regulating the proneurogenic transcription factor code that controls cortical neuron differentiation. In particular, we show here that the CB_1 receptor (1) tunes the differentiation balance of deep- and upper-layer cortical projection neurons, (2) is coupled to the regulation of the Ctip2–Satb2 transcriptional regulatory code, (3) plays a regulatory role in CSMNs development, and, as a consequence, (4) is required for the correct function of the mature CNS. Thus, cortical development is regulated by CB_1 receptor signaling through a dual progenitor-dependent and progenitor-independent mechanism of action. Although the CB_1 receptor present in neural progenitors promotes cortical progenitor self-renewal and VZ/SVZ proliferation in a cell-autonomous manner (Aguado et al., 2005; Mulder et al., 2008), the CB_1 receptor expressed in radially migrating neuroblasts controls the intrinsic neurogenic transcriptional program involved in the appropriate balance of cortical layer differentiation (present study) by sensing the extracellular eCB neurogenic niche.

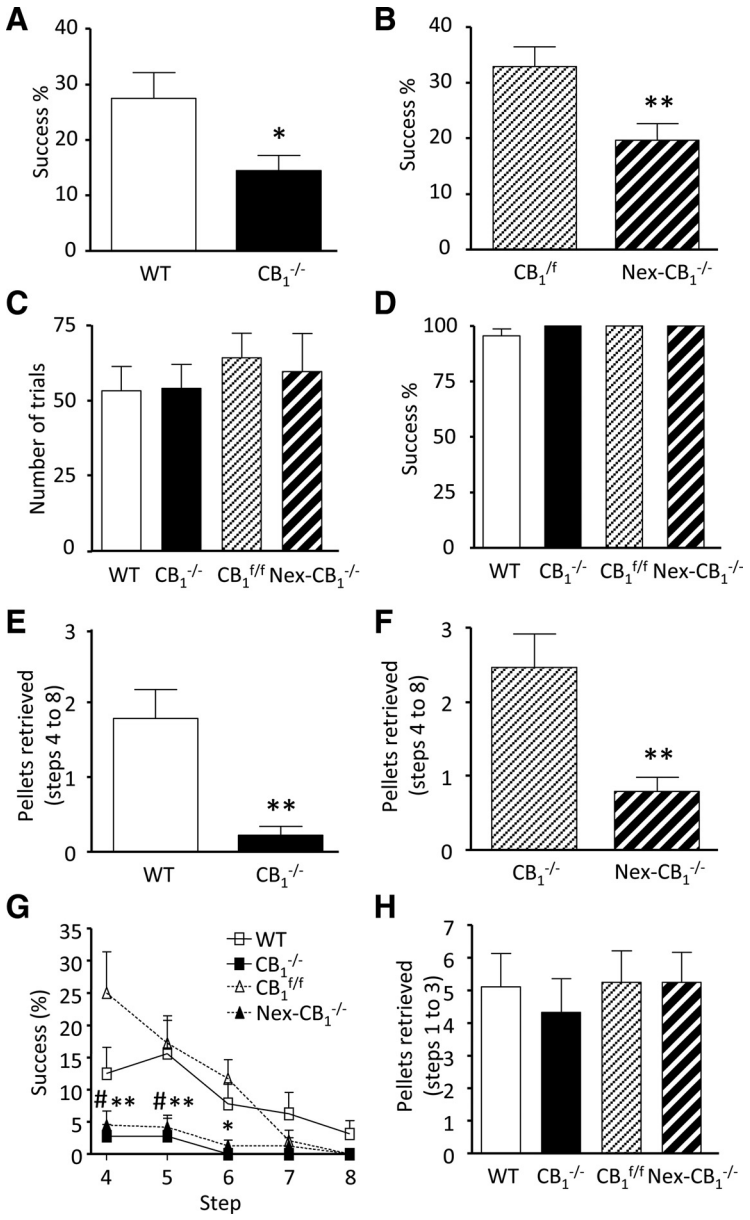

Figure 9. CB_1-deficient mice show impaired corticospinal motor function. ***A–C***, $CB_1^{-/-}$, *Nex–*$CB_1^{-/-}$, and their corresponding wild-type littermates (WT and $CB_1^{f/f}$, plain and stripped, black and white bars, respectively) were analyzed in the skilled pellet-reaching task test. Fine motor skill was evaluated in the animal groups after cage habituation and training. The percentage of pellets retrieved (***A***, ***B***) and the total number of trials performed during the skilled task (***C***) are shown. ***D***, Unskilled motor function was assessed, and the percentage of pellets retrieved was calculated. ***E***, ***F***, Mice were subjected to the staircase pellet-reaching test, and the sum of pellets retrieved from challenging steps (from 4–8) was compared between $CB_1^{-/-}$ or *Nex–*$CB_1^{-/-}$ mice and their control littermates. ***G***, The percentage of success for each step among the different genotypes was quantified. ***H***, The number of pellets reached in non-challenging steps 1–3 did not differ between groups. $n = 9$ ($CB_1^{-/-}$ and WT) and $n = 17$ and 16 (*Nex–*$CB_1^{-/-}$ and $CB_1^{f/f}$) for each group. $^*p < 0.05$, $^{**}p < 0.01$ versus WT, $^{\#}p < 0.05$ versus $CB_1^{f/f}$ littermates.

CB_1 cannabinoid receptor-dependent regulation of the neurogenic niche during neocortical development

During early cortical development, the CB_1 receptor is not expected to exert the classical neuromodulatory role of the eCB system in the mature adult brain, because synaptic maturation and activity is not yet completed. Therefore, during corticogenesis, CB_1 receptor-mediated neural fate decisions occur in a cell-autonomous manner (Aguado et al., 2005, 2007). Later, CB_1 receptor regulation of synaptic plasticity may turn a predominant mechanism of action, as exemplified at postnatal stages when the CB_1 receptor regulates the whisker map development of the somatosensory cortex in a neuronal activity-dependent manner (Li et al., 2009).

Here, we demonstrate that the CB_1 receptor allows differentiating neurons to transduce information from the surrounding neurogenic niche by modulating the intrinsic fate determinants involved in the developmental gene expression program of neuronal differentiation. It remains to be determined which signals control the production of eCBs released by neural progenitors and differentiating neurons (Aguado et al., 2005). Cortical progenitors express the enzyme involved in the synthesis of 2-arachidonoylglycerol (2AG) diacylglycerol lipase (Berghuis et al., 2007), which is downregulated during progenitor cell differentiation (Walker et al., 2010). In addition, the expression of the degradation enzymes FAAH and monoacylglycerol lipase (MAGL) during embryonic neuronal differentiation allows the delicate control of eCB levels (Aguado et al., 2005; Mulder et al.,

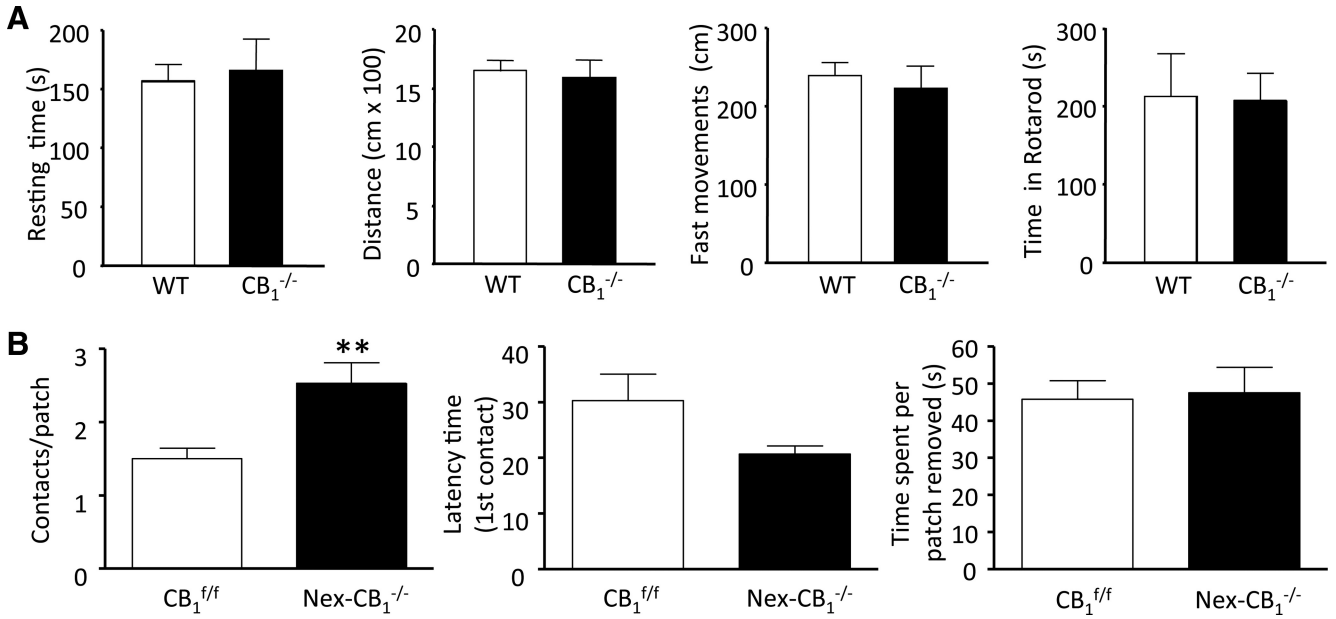

Figure 10. Behavioral characterization of $CB_1^{-/-}$ and $Nex–CB_1^{-/-}$ mice. ***A***, General motor behavior in $CB_1^{-/-}$ mice and WT littermates. Adult mice were analyzed for ambulation in the open-field test and for motor coordination in the RotaRod test. $n = 9$ for each group. ***B***, Patch-removal analysis confirms the deficient fine motor function of $Nex–CB_1^{-/-}$ mice compared with their $CB_1^{f/f}$ littermates. The number of contacts required for patch removal, the latency time for the first patch contact, and the time spent per patch were quantified in each genotype. $n = 16$ and 17 for each group. $^{**}p < 0.01$ versus $CB1^{f/f}$ mice.

2008; Keimpema et al., 2010). Regulation of 2AG availability by MAGL is responsible for the regulation of axonal growth by CB_1 receptor signaling (Keimpema et al., 2010). 2AG produced in thalamocortical axons can activate the CB_1 receptor present on growth cones of corticothalamic tracts, thus contributing to their correct integration and coordination (Wu et al., 2010). In addition, eCB depletion by the overexpression of the FAAH enzyme inhibits radial migration, suggesting a role of the endogenous cannabinoid tone in pyramidal neuron migration (Mulder et al., 2008). Overall, these evidences indicate that regulated expression and activity of the different signaling elements of the eCB system are part of the differentiation program of projection neurons.

CB_1 cannabinoid receptor-dependent regulation of forebrain neurogenic transcription network drives CSMN differentiation

Analyses of CB_1-deficient mice revealed that neuronal differentiation is altered, as shown by the delayed distribution of postmitotic $Tbr1^+$ neuroblasts and fate decision changes mediated by the Ctip2/Satb2 code. Nex–Cre-driven deletion of CB_1 allowed us to dissect the role of CB_1 solely in neuronal differentiation because, in $Nex–CB_1^{-/-}$ mice, cortical progenitors preserve CB_1 receptor expression and cell proliferation is not affected. The prominent role of the gene expression program regulated by the Ctip2 pathway in subcerebral CSMN generation (Arlotta et al., 2005; Chen et al., 2008; Tomassy et al., 2010) and the ability of the CB_1 receptor to control this transcriptional regulation axis reveal that the CB_1 receptor constitutes a novel signaling platform involved in the appropriate corticofugal neuronal development and skilled motor function by tuning subcerebral-projecting versus callosal neuron-projecting differentiation.

In $CB_1^{-/-}$ mice, the transcriptional repressor Satb2 is deregulated and $Satb2^+$ cells are expanded and occupy developing deep layers, in which they are normally absent (Alcamo et al., 2008; Britanova et al., 2008). Because of the inhibitory effect of Satb2 on Ctip2 expression (Alcamo et al., 2008; Britanova et al., 2008), CB_1 receptor deletion led to a reduction of $Ctip2^+$ cells generated in layer 5. These results suggest the existence of complementary changes in transcriptional regulators of CSMN specification during CB_1 receptor loss. In CB_1-deficient mice, reduced Ctip2 and Fezf2 expression was observed. Fezf2 acts upstream of Ctip2 and is necessary and sufficient to induce subcortical axonal projection neurons of deep cortical layers (Molyneaux et al., 2005; Chen et al., 2008). Upper-layer neurons develop normally with concomitant Fezf2 downregulation, whereas its overexpression induces the excessive generation of corticospinal projections from where callosal projections normally arise (Molyneaux et al., 2005). Of importance, Tbr1 and Fezf2 mutually repress each other, and this regulatory mechanism is essential for the development of the corticospinal tract (McKenna et al., 2011). Thus, alterations of the Tbr1–Fezf2 transcriptional balance may also contribute to the deficits in CSMN specification observed in the absence of CB_1 receptor signaling. In addition, loss of CB_1 receptor also affected Clim1, another member of the subcerebral specification transcriptional regulation program that allows distinction between callosal and subcerebral layer 5 projection neurons (Azim et al., 2009). Of note, our findings of unbalanced transcriptional regulation of projection neuron differentiation *in vivo* are supported by *in vitro* studies of CB_1 receptor-induced regulation of transcriptional activity and neuronal differentiation. Considering our previous data supporting a role of the eCB system in radial migration during corticogenesis (Mulder et al., 2008) and its ability to regulate downstream signaling systems that coordinate cell migration and neural cell differentiation, such as the mammalian target of rapamycin signaling pathway (Puighermanal et al., 2009; Palazuelos et al., 2012), a plausible hypothesis to be tested in the future would be the potential relationship between CB_1 receptor regulation of radial migration and neuronal differentiation.

Role of the CB_1 cannabinoid receptor in CSMN development and function: pathophysiological implications

Elucidating the contribution of CB_1 receptor expressed during brain development to the function of the future adult brain is a challenging task with important biomedical implications. In the present study, we provide evidence for the existence of functional impairments in the brains of adult CB_1 receptor-deficient mice as a consequence of alterations in developmental neuronal differentiation. Adult $CB_1^{-/-}$ mice show defective skilled motor function that ensues alterations of corticospinal tract development associated with the regulatory role of the CB_1 receptor of Ctip2/Satb2 transcriptional activity. Skilled motor behavior relies on the establishment of appropriate corticospinal connectivity, and even relatively mild alterations of the corticospinal tract can critically impair fine motor skills (Tomassy et al., 2010).

In addition to the skilled motor phenotype described herein, an emerging scenario suggests that genetic alterations or polymorphisms of CB_1 and eCB-synthesizing/degrading enzymes can contribute to changes, often subtle, in forebrain development, which might in turn contribute to the susceptibility to a variety of psychiatric disorders in the adult brain (Galve-Roperh et al., 2009; Fiskerstrand et al., 2010). Likewise, changes in prenatal CB_1 receptor function may conceivably ensue during pregnancy during mother's consumption of cannabinoid receptor agonists or antagonists (Jutras-Aswad et al., 2009) or exposure to other xenobiotics that interact with the eCB system, such as ethanol or organophosphorous pesticides (Nomura et al., 2008). Human and animal model studies have shown that loss of function of neuronal specification determinants (e.g., Tbr1, Satb2, Ctip2) results in alterations of cortical development and neurogenesis, which produces in the adult brain severe consequences in behavioral processes, such as motor control, cognition, epileptogenesis, and sensorimotor integration (Tomassy et al., 2010; Saito et al., 2011). Deregulated gene expression levels of deep-neuronal specification factors are associated with temporal lobe epilepsy and a particular form of autism (Pasca et al., 2011; Rossini et al., 2011).

Defective genesis and maturation of glutamatergic projection neurons alter the excitation/inhibition neurochemical balance and influence the interneuron populations of the cortical plate (Sessa et al., 2010; Lodato et al., 2011), and these alterations could contribute to the etiology of a large variety of disorders, such as epilepsy and schizophrenia (Lewis and Sweet, 2009). The participation of the CB_1 receptor in deep-layer neuronal differentiation and function reported here may provide a better understanding of the potential involvement of the eCB system in the neurodevelopmentally evoked susceptibility to motor neurodegenerative disorders (Blazquez et al., 2011), seizure occurrence (Marsicano et al., 2003), and psychiatric disorders (Jutras-Aswad et al., 2009).

References

Aguado T, Monory K, Palazuelos J, Stella N, Cravatt B, Lutz B, Marsicano G, Kokaia Z, Guzmán M, Galve-Roperh I (2005) The endocannabinoid system drives neural progenitor proliferation. FASEB J 19:1704–1706. CrossRef Medline

Aguado T, Romero E, Monory K, Palazuelos J, Sendtner M, Marsicano G, Lutz B, Guzmán M, Galve-Roperh I (2007) The CB1 cannabinoid receptor mediates excitotoxicity-induced neural progenitor proliferation and neurogenesis. J Biol Chem 282:23892–23898. CrossRef Medline

Alcamo EA, Chirivella L, Dautzenberg M, Dobreva G, Fariñas I, Grosschedl R, McConnell SK (2008) Satb2 regulates callosal projection neuron identity in the developing cerebral cortex. Neuron 57:364–377. CrossRef Medline

Arlotta P, Molyneaux BJ, Chen J, Inoue J, Kominami R, Macklis JD (2005) Neuronal subtype-specific genes that control corticospinal motor neuron development in vivo. Neuron 45:207–221. CrossRef Medline

Azim E, Shnider SJ, Cederquist GY, Sohur US, Macklis JD (2009) Lmo4 and Clim1 progressively delineate cortical projection neuron subtypes during development. Cereb Cortex 19 [Suppl 1]:i62–i69. CrossRef

Berghuis P, Rajnicek AM, Morozov YM, Ross RA, Mulder J, Urbán GM, Monory K, Marsicano G, Matteoli M, Canty A, Irving AJ, Katona I, Yanagawa Y, Rakic P, Lutz B, Mackie K, Harkany T (2007) Hardwiring the brain: endocannabinoids shape neuronal connectivity. Science 316:1212–1216. CrossRef Medline

Blázquez C, Chiarlone A, Sagredo O, Aguado T, Pazos MR, Resel E, Palazuelos J, Julien B, Salazar M, Börner C, Benito C, Carrasco C, Diez-Zaera M, Paoletti P, Díaz-Hernández M, Ruiz C, Sendtner M, Lucas JJ, de Yébenes JG, Marsicano G, et al. (2011) Loss of striatal type 1 cannabinoid receptors is a key pathogenic factor in Huntington's disease. Brain 134:119–136. CrossRef Medline

Britanova O, de Juan Romero C, Cheung A, Kwan KY, Schwark M, Gyorgy A, Vogel T, Akopov S, Mitkovski M, Agoston D, Sestan N, Molnár Z, Tarabykin V (2008) Satb2 is a postmitotic determinant for upper-layer neuron specification in the neocortex. Neuron 57:378–392. CrossRef Medline

Brooks SP, Dunnett SB (2009) Tests to assess motor phenotype in mice: a user's guide. Nat Rev Neurosci 10:519–529. CrossRef Medline

Chen B, Wang SS, Hattox AM, Rayburn H, Nelson SB, McConnell SK (2008) The Fezf2-Ctip2 genetic pathway regulates the fate choice of subcortical projection neurons in the developing cerebral cortex. Proc Natl Acad Sci U S A 105:11382–11387. CrossRef Medline

Cravatt BF, Demarest K, Patricelli MP, Bracey MH, Giang DK, Martin BR, Lichtman AH (2001) Supersensitivity to anandamide and enhanced endogenous cannabinoid signaling in mice lacking fatty acid amide hydrolase. Proc Natl Acad Sci U S A 98:9371–9376. CrossRef Medline

Feng G, Mellor RH, Bernstein M, Keller-Peck C, Nguyen QT, Wallace M, Nerbonne JM, Lichtman JW, Sanes JR (2000) Imaging neuronal subsets in transgenic mice expressing multiple spectral variants of GFP. Neuron 28:41–51. CrossRef Medline

Fishell G, Hanashima C (2008) Pyramidal neurons grow up and change their mind. Neuron 57:333–338. CrossRef Medline

Fiskerstrand T, H'mida-Ben Brahim D, Johansson S, M'zahem A, Haukanes BI, Drouot N, Zimmermann J, Cole AJ, Vedeler C, Bredrup C, Assoum M, Tazir M, Klockgether T, Hamri A, Steen VM, Boman H, Bindoff LA, Koenig M, Knappskog PM (2010) Mutations in ABHD12 cause the neurodegenerative disease PHARC: an inborn error of endocannabinoid metabolism. Am J Hum Genet 87:410–417. CrossRef Medline

Galve-Roperh I, Palazuelos J, Aguado T, Guzmán M (2009) The endocannabinoid system and the regulation of neural development: potential implications in psychiatric disorders. Eur Arch Psychiatry Clin Neurosci 259:371–382. CrossRef Medline

Guillemot F, Molnár Z, Tarabykin V, Stoykova A (2006) Molecular mechanisms of cortical differentiation. Eur J Neurosci 23:857–868. CrossRef Medline

Han W, Kwan KY, Shim S, Lam MM, Shin Y, Xu X, Zhu Y, Li M, Sestan N (2011) TBR1 directly represses Fezf2 to control the laminar origin and development of the corticospinal tract. Proc Natl Acad Sci U S A 108:3041–3046. CrossRef Medline

Harkany T, Guzmán M, Galve-Roperh I, Berghuis P, Devi LA, Mackie K (2007) The emerging functions of endocannabinoid signaling during CNS development. Trends Pharmacol Sci 28:83–92. CrossRef Medline

Hevner RF, Shi L, Justice N, Hsueh Y, Sheng M, Smiga S, Bulfone A, Goffinet AM, Campagnoni AT, Rubenstein JL (2001) Tbr1 regulates differentiation of the preplate and layer 6. Neuron 29:353–366. CrossRef Medline

Jutras-Aswad D, DiNieri JA, Harkany T, Hurd YL (2009) Neurobiological consequences of maternal cannabis on human fetal development and its neuropsychiatric outcome. Eur Arch Psychiatry Clin Neurosci 259:395–412. CrossRef Medline

Keimpema E, Barabas K, Morozov YM, Tortoriello G, Torii M, Cameron G, Yanagawa Y, Watanabe M, Mackie K, Harkany T (2010) Differential subcellular recruitment of monoacylglycerol lipase generates spatial specificity of 2-arachidonoyl glycerol signaling during axonal pathfinding. J Neurosci 30:13992–14007. CrossRef Medline

Lai T, Jabaudon D, Molyneaux BJ, Azim E, Arlotta P, Menezes JR, Macklis JD (2008) SOX5 controls the sequential generation of distinct corticofugal neuron subtypes. Neuron 57:232–247. CrossRef Medline

Lewis DA, Sweet RA (2009) Schizophrenia from a neural circuitry perspec-

tive: advancing toward rational pharmacological therapies. J Clin Invest 119:706–716. CrossRef Medline

Li L, Bender KJ, Drew PJ, Jadhav SP, Sylwestrak E, Feldman DE (2009) Endocannabinoid signaling is required for development and critical period plasticity of the whisker map in somatosensory cortex. Neuron 64: 537–549. CrossRef Medline

Lodato S, Rouaux C, Quast KB, Jantrachotechatchawan C, Studer M, Hensch TK, Arlotta P (2011) Excitatory projection neuron subtypes control the distribution of local inhibitory interneurons in the cerebral cortex. Neuron 69:763–779. CrossRef Medline

Marsicano G, Goodenough S, Monory K, Hermann H, Eder M, Cannich A, Azad SC, Cascio MG, Gutiérrez SO, van der Stelt M, López-Rodriguez ML, Casanova E, Schütz G, Zieglgänsberger W, Di Marzo V, Behl C, Lutz B (2003) CB1 cannabinoid receptors and on-demand defense against excitotoxicity. Science 302:84–88. CrossRef Medline

Massa F, Mancini G, Schmidt H, Steindel F, Mackie K, Angioni C, Oliet SH, Geisslinger G, Lutz B (2010) Alterations in the hippocampal endocannabinoid system in diet-induced obese mice. J Neurosci 30:6273–6281. CrossRef Medline

McKenna WL, Betancourt J, Larkin KA, Abrams B, Guo C, Rubenstein JL, Chen B (2011) Tbr1 and Fezf2 regulate alternate corticofugal neuronal identities during neocortical development. J Neurosci 31:549–564. CrossRef Medline

Molyneaux BJ, Arlotta P, Hirata T, Hibi M, Macklis JD (2005) Fezl is required for the birth and specification of corticospinal motor neurons. Neuron 47:817–831. CrossRef Medline

Molyneaux BJ, Arlotta P, Menezes JR, Macklis JD (2007) Neuronal subtype specification in the cerebral cortex. Nat Rev Neurosci 8:427–437. CrossRef Medline

Monory K, Massa F, Egertová M, Eder M, Blaudzun H, Westenbroek R, Kelsch W, Jacob W, Marsch R, Ekker M, Long J, Rubenstein JL, Goebbels S, Nave KA, During M, Klugmann M, Wölfel B, Dodt HU, Zieglgänsberger W, Wotjak CT, et al. (2006) The endocannabinoid system controls key epileptogenic circuits in the hippocampus. Neuron 51:455–466. CrossRef Medline

Monory K, Blaudzun H, Massa F, Kaiser N, Lemberger T, Schütz G, Wotjak CT, Lutz B, Marsicano G (2007) Genetic dissection of behavioural and autonomic effects of Delta(9)-tetrahydrocannabinol in mice. PLoS Biol 5:e269. CrossRef Medline

Morozov YM, Torii M, Rakic P (2009) Origin, early commitment, migratory routes, and destination of cannabinoid type 1 receptor-containing interneurons. Cereb Cortex 19 [Suppl 1]:i78–i89. CrossRef

Mulder J, Aguado T, Keimpema E, Barabás K, Ballester Rosado CJ, Nguyen L, Monory K, Marsicano G, Di Marzo V, Hurd YL, Guillemot F, Mackie K, Lutz B, Guzmán M, Lu HC, Galve-Roperh I, Harkany T (2008) Endocannabinoid signaling controls pyramidal cell specification and long-range axon patterning. Proc Natl Acad Sci U S A 105:8760–8765. CrossRef Medline

Nomura DK, Blankman JL, Simon GM, Fujioka K, Issa RS, Ward AM, Cravatt BF, Casida JE (2008) Activation of the endocannabinoid system by organophosphorus nerve agents. Nat Chem Biol 4:373–378. CrossRef Medline

Palazuelos J, Ortega Z, Díaz-Alonso J, Guzmán M, Galve-Roperh I (2012) CB2 cannabinoid receptors promote neural progenitor cell proliferation via mTORC1 signaling. J Biol Chem 287:1198–1209. CrossRef Medline

Paşca SP, Portmann T, Voineagu I, Yazawa M, Shcheglovitov A, Paşca AM, Cord B, Palmer TD, Chikahisa S, Nishino S, Bernstein JA, Hallmayer J, Geschwind DH, Dolmetsch RE (2011) Using iPSC-derived neurons to uncover cellular phenotypes associated with Timothy syndrome. Nat Med 17:1657–1662. CrossRef Medline

Puighermanal E, Marsicano G, Busquets-Garcia A, Lutz B, Maldonado R, Ozaita A (2009) Cannabinoid modulation of hippocampal long-term memory is mediated by mTOR signaling. Nat Neurosci 12:1152–1158. CrossRef Medline

Rossini L, Moroni RF, Tassi L, Watakabe A, Yamamori T, Spreafico R, Garbelli R (2011) Altered layer-specific gene expression in cortical samples from patients with temporal lobe epilepsy. Epilepsia 52:1928–1937. CrossRef Medline

Saito T, Hanai S, Takashima S, Nakagawa E, Okazaki S, Inoue T, Miyata R, Hoshino K, Akashi T, Sasaki M, Goto Y, Hayashi M, Itoh M (2011) Neocortical layer formation of human developing brains and lissencephalies: consideration of layer-specific marker expression. Cereb Cortex 21: 588–596. CrossRef Medline

Schneider M (2009) Cannabis use in pregnancy and early life and its consequences: animal models. Eur Arch Psychiatry Clin Neurosci 259:383–393. CrossRef Medline

Sessa A, Mao CA, Colasante G, Nini A, Klein WH, Broccoli V (2010) Tbr2-positive intermediate (basal) neuronal progenitors safeguard cerebral cortex expansion by controlling amplification of pallial glutamatergic neurons and attraction of subpallial GABAergic interneurons. Genes Dev 24:1816–1826. CrossRef Medline

Sur M, Rubenstein JL (2005) Patterning and plasticity of the cerebral cortex. Science 310:805–810. CrossRef Medline

Tomassy GS, De Leonibus E, Jabaudon D, Lodato S, Alfano C, Mele A, Macklis JD, Studer M (2010) Area-specific temporal control of corticospinal motor neuron differentiation by COUP-TFI. Proc Natl Acad Sci U S A 107:3576–3581. CrossRef Medline

Walker DJ, Suetterlin P, Reisenberg M, Williams G, Doherty P (2010) Down-regulation of diacylglycerol lipase-alpha during neural stem cell differentiation: identification of elements that regulate transcription. J Neurosci Res 88:735–745. CrossRef Medline

Wu CS, Zhu J, Wager-Miller J, Wang S, O'Leary D, Monory K, Lutz B, Mackie K, Lu HC (2010) Requirement of cannabinoid CB(1) receptors in cortical pyramidal neurons for appropriate development of corticothalamic and thalamocortical projections. Eur J Neurosci 32:693–706. CrossRef Medline

Wu SX, Goebbels S, Nakamura K, Nakamura K, Kometani K, Minato N, Kaneko T, Nave KA, Tamamaki N (2005) Pyramidal neurons of upper cortical layers generated by NEX-positive progenitor cells in the subventricular zone. Proc Natl Acad Sci U S A 102:17172–17177. CrossRef Medline